1970

Elastic Stress Distribution in Square Plates Weakened by a Large Central Elliptical or Circular Notch

Sameh M. Kanan

ELASTIC STRESS DISTRIBUTION IN SQUARE PLATES WEAKENED BY A LARGE CENTRAL ELLIPTICAL OR CIRCULAR NOTCH

BY

SAMEH M. KANAN

A thesis submitted
in partial fulfillment of the requirements for the
degree Master of Science, Major in
Civil Engineering, South Dakota
State University

1970

ELASTIC STRESS DISTRIBUTION IN SQUARE PLATES WEAKENED BY A LARGE CENTRAL ELLIPTICAL OR CIRCULAR NOTCH

This thesis is approved as a creditable and independent investigation by a candidate for the degree, Master of Science, and is acceptable as meeting the thesis requirements for this degree, but without implying that the conclusions reached by the candidate are necessarily the conclusions of the major department.

Thesis Adviser   Date

Head, Civil Engineering Department   Date

ACKNOWLEDGEMENTS

The author wishes to express his deep gratitude to Dr. Zaher Shoukry, Associate Professor, Department of Civil Engineering, for his great assistance and for his encouragement in developing and analyzing the course of this research project. To him the author is truly indebted.

This thesis is dedicated to the author's mother and father for their deep encouragement and long sacrifice.

SMK

TABLE OF CONTENTS

LIST OF FIGURES

CHAPTER I

INTRODUCTION

A. General

The extensive use of steel and high-strength alloys led to types of structures embodying slender compression members, thin plates, and thin shells. This fact has made elastic instability a problem of great importance. Urgent practical requirements have given rise in recent years to extensive investigation, both theoretical and experimental, of the elastic stress distribution in such structural elements as bars, plates, and shells. This is of particular importance because the analysis of elastic stress distribution is the first step in the investigation of the critical loads. The stress analysis becomes very complicated with the introduction of a notch in a compression slender member. Often notches are introduced into the design of a structural member to allow the passage of electrical wire bundles, hydraulic and air conduits, or other structural members. A notch may also serve as an inspection access opening.

The mathematical solution for determining the elastic stress distribution in a plate requires that equilibrium and boundary conditions be satisfied. This can be accomplished by integration of the equilibrium partial

differential equations of the flat plate. As the nature of a notched plate problem prohibits an easy solution in a closed form, a numerical technique is hereby attempted. The finite difference method is one of the widely accepted methods for such analysis and is the method chosen for this investigation.

B. Historical Background

> "Even a brief reading of any text on plates and shells reveals that some half or more of the work is devoted to finding approximations and substitutions which will lead to analytical solutions for a particular problem. Until the recent past, such solutions were necessary if the theory was to be used at all. Even now these solutions are welcome where brief or simple solutions emerge. Such cases are, however, relatively rare and the widespread use of electronic digital computers to provide a direct numerical answer has, in part, superseded the need for involved solutions in terms of advanced mathematical functions."[1]

The above statement explains the reasons why the problem of notched plates has been avoided until the recent past. Nowadays, with the availability of electronic computers and with the application of numerical techniques, investigators are attempting to solve complicated problems that they avoided in the past.

---

[1]C. E. Turner, Introduction to Plate and Shell Theory (American Elsevier Publishing Company, Inc., New York, 1965), p. x.

Shoukry[2] employed the method of finite differences to investigate the stress distribution in and the buckling characteristics of the webs of castellated steel beams. The results obtained indicated that the elastic stress distribution was accurate for the relatively fine mesh used (18 X 10).

Hoffman[3] investigated with a similar procedure the stress distribution in a plate with a side notch. His results showed that the finite difference method employed for stress distribution analysis had given relatively accurate results.

Kanan[4] investigated the elastic stress distribution in a rectangularly notched plate axially loaded by uniform compression. His results confirmed that the finite difference method had given relatively accurate results, considering the complexities of the problem treated.

---

[2] Z. Shoukry, "Elastic Flexural Stress Distribution in Webs of Castellated Steel Beams," Welding Journal, American Welding Society, Vol. 64 (May 1965), p. 231-s.

[3] P. Hoffman, "Elastic Stress Distribution in Rectangularly Notched Members," (unpublished Master of Science Thesis, South Dakota State University, Brookings, South Dakota, 1965).

[4] M. Kanan, "Elastic Stress Distribution in and Stability of Rectangularly Notched Plates Axially Loaded by Uniform Compression," (unpublished Master of Science Thesis, South Dakota State University, Brookings, South Dakota, 1967).

Other investigators employed the method of finite differences successfully when investigating stress distribution in deep beams.[5,6,7] They concluded that the results are excellent as long as a relatively fine mesh is employed. Also, these results indicated that the agreement between the finite difference method and a more accurate function solution in a closed form was good, even for a relatively coarse mesh.

White and Cottingham[8] investigated the critical buckling loads in and the stability of solid plates partially loaded at the ends. They concluded that the use of the finite difference method for determining elastic buckling loads is satisfactorily accurate. They also found that increased accuracy can be obtained by using a relatively fine mesh subdivision.

---

[5] L. Chow, H. D. Conway and G. Winter, "Stress in Deep Beams," Transactions, American Society of Civil Engineers, Vol. 118 (1963), p. 686.

[6] F. Geer, "Stresses in Deep Beams," Journal of the American Concrete Institute, Vol. 56 (1960), p. 151.

[7] H. D. Conway, L. Chow, and G. W. Morgan, "Analysis of Deep Beams," Journal of Applied Mechanics, Vol. 18 (1951), p. 686.

[8] R. N. White and W. S. Cottingham, "Stability of Plates Under Partial Edge Loading," Proceedings, American Society of Civil Engineers, Engineering Mechanics Division, No. 3297, Vol. 88 (October, 1962).

C. Object and Scope of Investigation

The main objective for this investigation is to examine the applicability of the finite difference method in obtaining the elastic stress distribution in a square plate weakened by a large elliptical or circular notch. A square mesh is used with maximum subdivisions as allowed by the storage capacity of the computer available at South Dakota State University. The nodal points of the mesh are placed in such a way as to give an approximate outline of the circular or elliptical shape.

The plates under study are simply supported along two edges and free along the other two, and subjected to uniform compression. Two types of notches are introduced at the center of the plate; one is circular and the other is elliptical in shape. With the aid of the electronic computer and the utilization of the finite difference technique principal stress contours in each plate are obtained. These stress contours for both the circular and the elliptical notches are compared. Such comparison will assist the structural designer in obtaining the more efficient type of notch.

The stress distribution analysis consists of computing the following:

(1) normal stresses acting in the x and y directions

(2) shearing stress acting on the xy-plane

(3) major and minor principal stresses and their orientations with respect to the x-axis.

These quantities are computed at each nodal point throughout the section of plate.

The finite difference computations are carried out with the aid of an electronic computer. The computer output for the stress distribution was printed out using a special board so that the results are shown on the actual plan shape of the plate section under consideration. This permitted stress contours to be drawn within the outline of the section.

The solutions presented in this work provide a valuable source of information for future investigations. This analysis is of particular importance in the determination of buckling loads for plates identical to those investigated in this study.

CHAPTER II

ELASTIC STRESS ANALYSIS

A. Choice of Analytical Method

In the elastic stress distribution analysis of a thin plate, where the dimensions of the plate are given in Cartesian coordinates, the ideal method of solution is to obtain an exact evaluation for the function ϕ which satisfies the biharmonic equation[9]:

$$\frac{\partial^4 \phi}{\partial x^4} + 2\frac{\partial^4 \phi}{\partial x^2 \partial y^2} + \frac{\partial^4 \phi}{\partial y^4} = 0 \qquad (1)$$

Where

ϕ = Airy's stress function

Equation (1) must be satisfied for any point within the domain of the plate. Once this is achieved, the stresses in the plate can be computed from the stress function ϕ according to the expressions[10]:

$$\sigma_x = \frac{\partial^2 \phi}{\partial y^2} \qquad (2)$$

---

[9] S. Timoshenko and J. N. Goodier, Theory of Elasticity, (McGraw-Hill Book Company, Incorporated, New York, New York, 1951), p. 26.

[10] Ibid.

$$\sigma_y = \frac{\partial^2 \phi}{\partial x^2} \tag{3}$$

$$\tau_{xy} = -\frac{\partial^2 \phi}{\partial x \partial y} \tag{4}$$

Where

σ_x = stress in the X-direction,

σ_y = stress in the Y-direction,

τ_{xy} = shearing stress in the X-Y plane.

Since the nature of the problem and the introduction of the notch in the plate prohibit an easy solution for equation (1), an approximate method of analysis is employed. The method chosen is the finite difference method.

> The finite difference technique[11] "essentially replaces the differential governing equations and the boundary conditions by finite differences approximations in terms of a finite number of unknown values of the dependent variables at a number of discrete points within or just outside the domain of integration. The finite differences equations form a set of linear algebraic equations to solve for the set of unknowns. The task of accomplishing such numerical solution of large numbers of simultaneous equations can be achieved by the aid of electronic computer."

---

[11] O. C. Zienkiewics and G. S. Holister, <u>Stress Analysis</u>, (John Wiley and Sons, Ltd., London, 1965), p. 7.

B. Plate Stress Distribution

The finite difference method essentially approximates partial differential equations by finite difference equations in the form of an "operator molecule".[12] Assuming a square network, the operator molecule for the biharmonic equation is[13]:

$$\nabla^4 \phi \simeq \frac{1}{h^4} \begin{bmatrix} & & 1 & & \\ & 2 & -8 & 2 & \\ 1 & -8 & 20 & -8 & 1 \\ & 2 & -8 & 2 & \\ & & 1 & & \end{bmatrix} \qquad (5)$$

in which "h" is the mesh spacing.

In the process of determining the stress function ϕ by this method, the domain of the plate is replaced by a

---

[12] P. C. Wang, Numerical and Matrix Methods in Structural Mechanics (John Wiley and Sons, Incorporated, New York, New York, 1966), pp. 50-52.

[13] S. H. Crandall, Engineering Analysis (McGraw-Hill Book Company, Incorporated, New York, New York, 1956), pp. 243-247.

mesh of individual nodal points of square spacing "h". The stress function values are then calculated for each discrete nodal point.

Once the values of the stress function at each point of the mesh system are found, the stresses corresponding to these values are then determined. The expressions for the stress components and their finite difference operator molecules are as follows:[14]

$$\sigma_x = \frac{\partial^2 \phi}{\partial y^2} \simeq +\frac{1}{h^2}\begin{bmatrix} 1 \\ -2 \\ 1 \end{bmatrix} \tag{6}$$

$$\sigma_y = \frac{\partial^2 \phi}{\partial x^2} \simeq +\frac{1}{h^2}\begin{bmatrix} 1 & -2 & 1 \end{bmatrix} \tag{7}$$

and

$$\tau_{xy} = -\frac{\partial^2 \phi}{\partial x \partial y} \simeq +\begin{bmatrix} -1 & 0 & 1 \\ 0 & 0 & 0 \\ 1 & 0 & -1 \end{bmatrix} \tag{8}$$

---

[14]S. Timoshenko and S. Woinowsky-Krieger, Theory of Plates and Shells, Second Edition (McGraw-Hill Book Company, Incorporated, New York, New York, 1959), p. 360.

The above molecules are employed by first placing each molecule's central value over each nodal point and then summing algebraically the terms resulting from the multiplication of each molecule's component by its corresponding stress function value. This summation gives the stress at each nodal point.

C. Boundary Value Problems

1. General

The values of the stress function at the boundary of a structural section depend upon the loading conditions applied at that boundary. Such values, which can be determined mathematically, are the controlling values for the stress function throughout the domain of the plate.

Since the biharmonic molecule must be satisfied when applied to each interior nodal point within the domain, initial stress function values are assigned for each nodal point. These values are then modified by an iterative technique to satisfy the biharmonic molecule. When the molecule is applied to interior points adjacent to the boundary, values of the stress function immediately outside the boundary are required. For this reason the stress function values for points outside the boundary are extrapolated from the stress function values on the boundary.

2. General Stress Function Boundary Equations

Consider a thin, homogeneous, isotropic square plate simply supported along two opposite edges, and free along the other two edges. The plate is subjected to a uniformly distributed uniaxial load, and is weakened by an elliptical cut-out, as shown in Figure 1.

The dimensions of the plate are as follows:

$2L$ = length of the plate

t = uniform thickness of the plate

$2a$ = major diameter of the elliptical notch

$2b$ = minor diameter of the elliptical notch

and

σ_n = axial compressive stress along side OA taken as 20 units for convenience.

Due to symmetry about the horizontal and vertical center-lines, only one quarter of the plate is considered for obtaining a solution for the boundary values of the stress function. The quarter plate is shown in Figure 2. This consideration allows the same number of nodal points dictated by the storage capacity of the computer to be distributed over a small area, and thus increasing the accuracy of the solution.

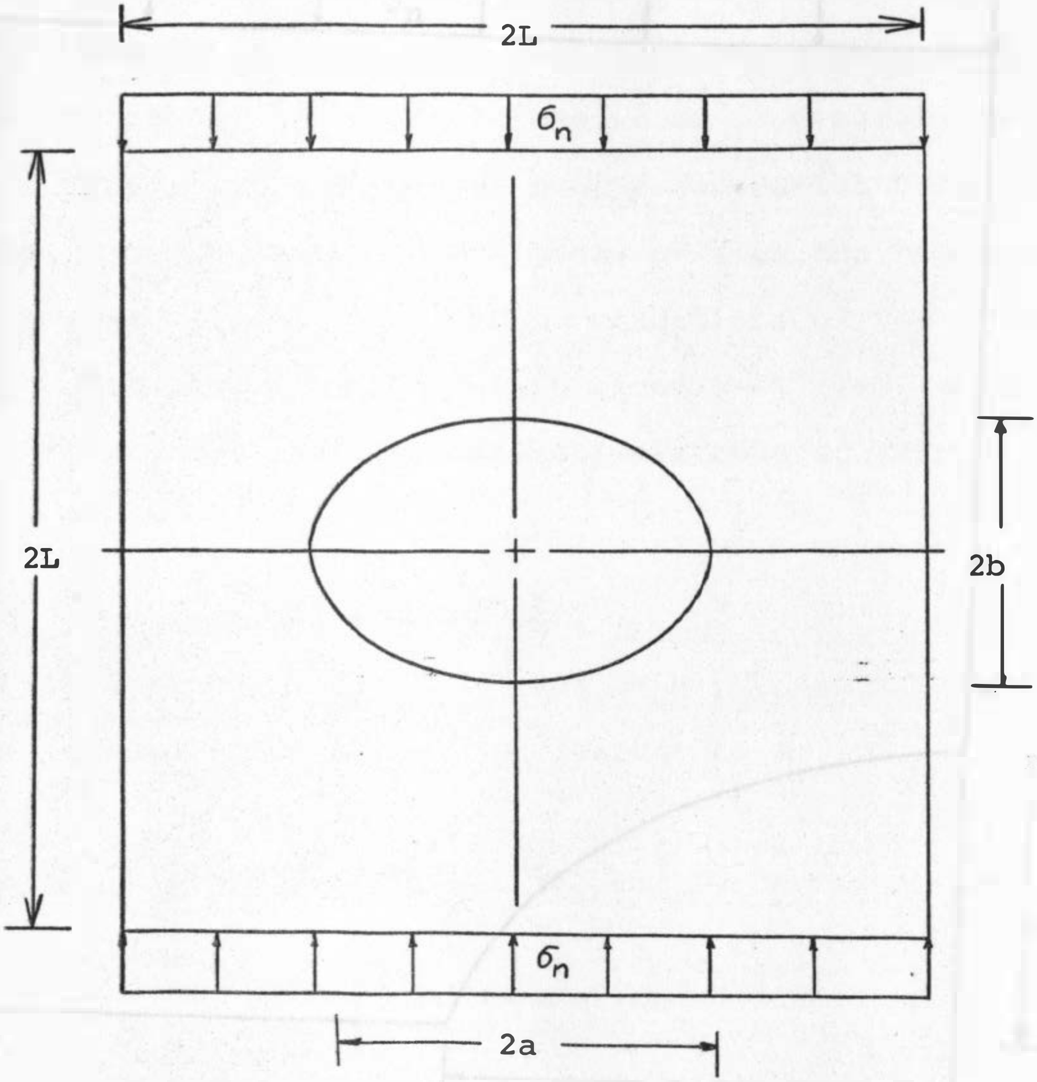

Figure 1. The Full Plate

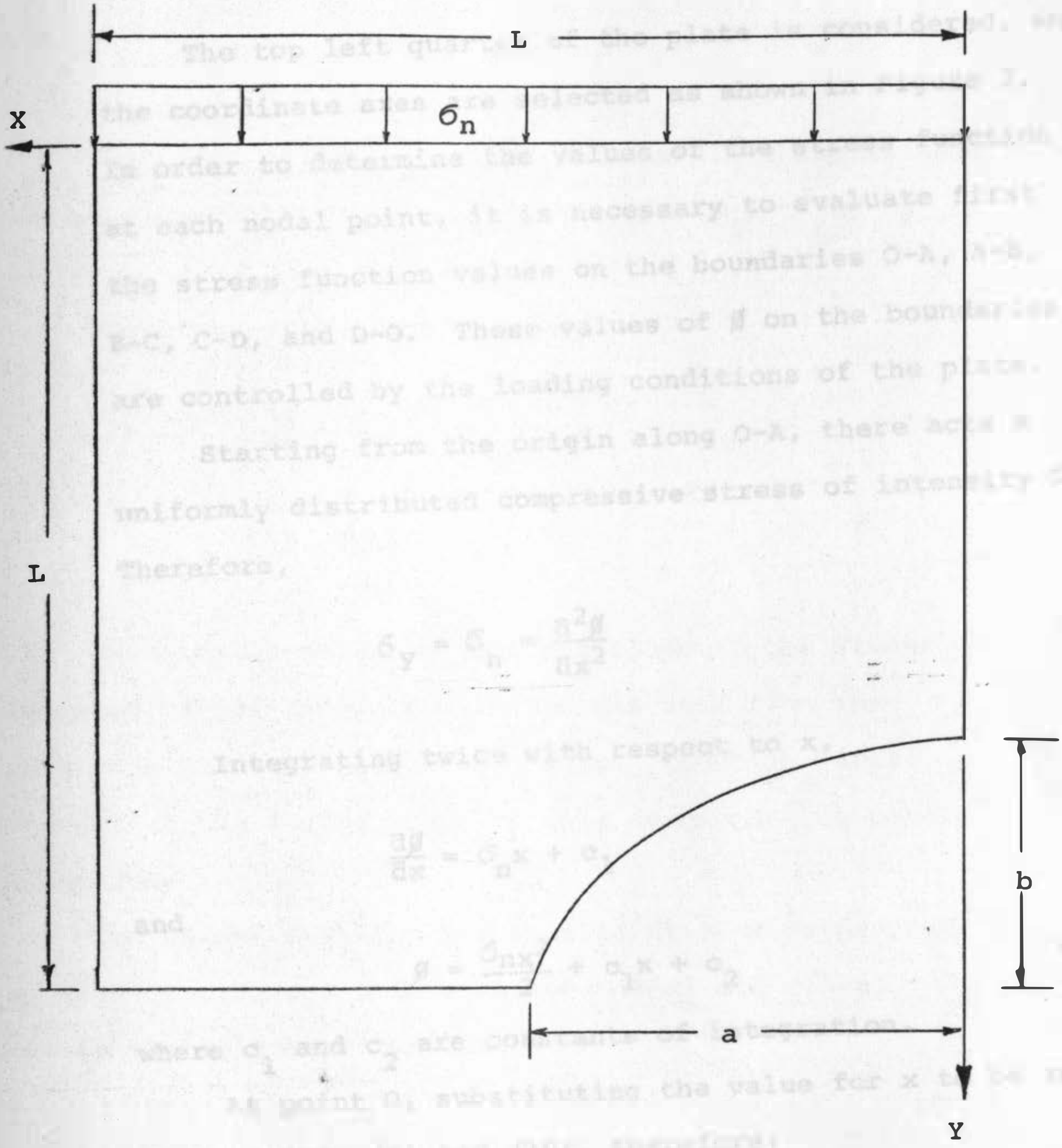

Figure 2. The Quarter Plate

The top left quarter of the plate is considered, and the coordinate axes are selected as shown in Figure 2. In order to determine the values of the stress function at each nodal point, it is necessary to evaluate first the stress function values on the boundaries O-A, A-B, B-C, C-D, and D-O. These values of $\emptyset$ on the boundaries are controlled by the loading conditions of the plate.

Starting from the origin along O-A, there acts a uniformly distributed compressive stress of intensity σ_n. Therefore,

$$\sigma_y = \sigma_n = \frac{d^2\emptyset}{dx^2}$$

Integrating twice with respect to x,

$$\frac{d\emptyset}{dx} = \sigma_n x + c_1 \tag{9}$$

and

$$\emptyset = \frac{\sigma_n x^2}{2} + c_1 x + c_2 \tag{10}$$

where c_1 and c_2 are constants of integration.

At point O, substituting the value for x to be zero in equations (9) and (10), therefore:

$$\frac{d\emptyset}{dx} = c_1$$

and

$$\emptyset = c_2$$

The terms c_1 and c_2 can be taken arbitrarily as zero values since point O is only a reference point for $\frac{d\emptyset}{dx}$ and $\emptyset$.

Therefore, along the boundary O-A,

$$\frac{d\emptyset}{dx} = \sigma_n x \tag{9-a}$$

and

$$\emptyset = \frac{\sigma_n x^2}{2} \tag{10-a}$$

Equation (9-a) shows that the slope of the stress function varies linearly with the distance from the reference point O, along the X-axis. Equation (10-a) shows that the stress function is a second degree parabola along O-A.

The stress function value at point A is determined by substituting x = L in equations (9-a) and (10-a), giving the following results:

$$\frac{d\emptyset}{dx} = \sigma_n L \tag{9-b}$$

and

$$\emptyset = \frac{\sigma_n L^2}{2} \tag{10-b}$$

Side A-B is a free boundary, and therefore:

$$\sigma_x = \frac{\partial^2 \phi}{\partial y^2} = 0$$

Integrating twice with respect to y,

$$\frac{\partial \phi}{\partial y} = c_3$$

and

$$\phi = c_3 y + c_4$$

But at point A, there are only normal stresses along the side O-A in the Y-direction. Hence,

$$\frac{\partial \phi}{\partial y} = 0$$

and

$$c_3 = 0$$

and the stress function value at point A reduces to the expression,

$$\phi = c_4$$

But, from equation (10-b), the value of the stress function, ϕ, at point A is given as $\frac{\sigma_n L^2}{2}$, therefore:

$$\phi = c_4 = \frac{\sigma_n L^2}{2} .$$

and along the boundary A-B,

$$\emptyset = \text{a constant, } c_4, = \frac{\sigma_n L^2}{2}$$

This indicates that the stress function along side A-B is constant and its value is equal to the value of the stress function at A as calculated along side O-A.

Along boundary B-C there acts a variable stress of unknown value. However, the stress function value at point B when obtained from boundary B-C has to be the same as the value obtained from boundary A-B. The stress function value at any other point on boundary B-C is obtained through the iteration process.

Along boundary C-D there are no stresses applied. Therefore, the value of the stress function at any point on this boundary must be the same as the value of the stress function at point C. This value at C is obtained from the iteration process, and the computer program is instructed to allocate this value to all points along the boundary C-D.

The stress acting along boundary D-O is unknown. Therefore, no attempt is made to evaluate the stress function along this boundary at this stage. However, the stress function along D-O is determined through the iteration process.

CHAPTER III

STRESS FUNCTION VALUES FORMULATION

A. Stress Function Values on the Boundary

In order to determine the values of the stress function at each nodal point along the boundaries, it is necessary to obtain the stress function equations for each boundary. These equations are derived in Chapter II. In the determination of the stress function equations, it was shown that the stress function depends upon the type of loading acting on the boundaries and on the support conditions of the boundaries. For the plates under investigation, the loading is uniformly distributed and acts along two opposite simply supported edges, while the other two edges are free. The value of the loading, σ_n, acting on the plates is taken as 20 units for convenience. The length for each side of the square plate is taken as 40h, where "h" is the nodal spacing. Thus, when considering the quarter plate, the length, L, of each quarter plate is equal to 20h. The value of the nodal spacing, h, is taken as unity to simplify mathematical calculations.

For determining the actual mathematical value of the stress function at each nodal point along the boundaries, values for "L", "h", and "σ_n" are substituted into

the stress function equations previously derived. The derivation of these equations is shown in full in Chapter II.

B. Stress Function Values Outside the Boundary

When the stress function operator molecule is applied to points immediately inside the boundary, the stress function values for the corresponding points outside the boundary are needed. This need arises from the fact that the operator molecule extends to two points on either side of the point to which the molecule is applied. The values of the stress function for points on the boundary are already determined. Therefore, it is necessary to obtain the stress function values for points immediately outside the boundary. This is accomplished either by extrapolation or by symmetry conditions.

Referring to Figure 3 , the values of the stress function immediately beyond the boundary O-A are considered to be identical to those on the boundary O-A itself. This assumption is valid since the member can be considered as a continuous plate. The value of $\emptyset$ at point A' beyond point A along the boundary O-A is determined by extrapolation of the second degree parabola for the stress function along O-A given by equation (10-a).

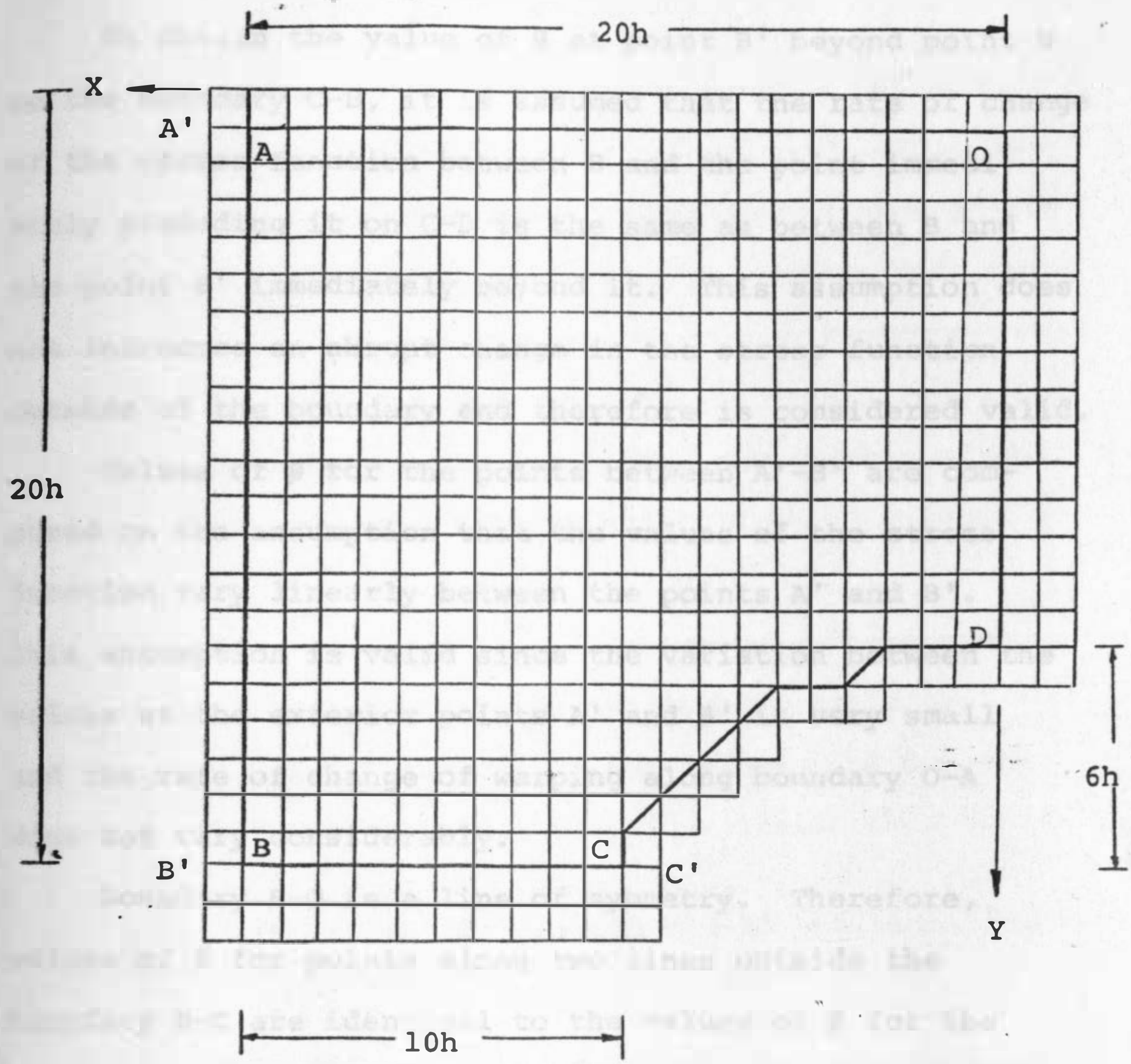

Figure 3. Quarter Plate - Mesh Subdivision

To obtain the value of Ø at point B' beyond point B on the boundary C-B, it is assumed that the rate of change of the stress function between B and the point immediately preceding it on C-B is the same as between B and the point B' immediately beyond it. This assumption does not introduce an abrupt change in the stress function outside of the boundary and therefore is considered valid.

Values of Ø for the points between A'-B' are computed on the assumption that the values of the stress function vary linearly between the points A' and B'. This assumption is valid since the variation between the values at the exterior points A' and B' is very small and the rate of change of warping along boundary O-A does not vary considerably.

Boundary B-C is a line of symmetry. Therefore, values of Ø for points along two lines outside the boundary B-C are identical to the values of Ø for the corresponding points along two lines inside this boundary.

To obtain the value of Ø at point C' beyond point C on boundary B-C, it is assumed that the rate of change of the stress function between C and the point immediately preceding it on B-C is the same as between C and C'. This assumption is the same as saying that the value of

the stress acting at point C is the same as the stress acting at the point immediately preceding C. This assumption would not introduce a significant error if the mesh spacing is small. Also, this assumption does not introduce any abrupt change in the stress function outside the boundary B-C and therefore is considered valid.

C-D is a free boundary. Therefore, values of the stress function outside the boundary C-D are assumed to be identical to the value of Ø at point C'.

Boundary D-O is a line of symmetry. Therefore, values of Ø for points along two lines outside the boundary D-O are identical to the values of Ø for the corresponding points along two lines inside this boundary.

C. Iterative Technique for Determining Interior Values of the Stress Function

After the equations for the boundary stress function values are obtained, the surface of the plate is replaced by a lattice of square spacing. The stress function values are then calculated for each discrete point on and immediately outside the boundaries whose stress function equations have been determined. Initial stress function values are assigned for each nodal point within the domain of the plate. At this stage, each discrete point has either a calculated stress function value or

an assigned value. This information is used as computer input.

An iterative technique is employed to satisfy the biharmonic operator molecule whenever this is applied to each interior nodal point and to points along the center-lines. By this technique the molecule is applied to every point on the plate, and the existing stress function value is replaced each time by a modified computed value. This process "forces" the stress function values on the iterated points to converge to suitable values dictated by the stress function values on and immediately outside the controlling fixed boundaries. As the convergence of the system continues, the biharmonic molecule becomes more nearly satisfied at each nodal point within the domain, and the residual for each nodal point iterated approaches zero.

The entire process is programmed in Fortran IV language for calculation on the IBM 360 electronic computer. The program is so constructed that two values are printed after each iteration. The first number is the largest difference between any two values obtained at any point in two successive iterations. The second number is the largest percentage of change between two successive iterations. These two numbers supply a visual

running check on the convergence of the system. The computer program for computing the stress function values for the circular notch is shown in Appendix A.

D. Determination of Stresses

Once the final values of the stress function $\emptyset$ are determined for all nodal points, the stresses σ_x, σ_y, and τ_{xy} are determined by their finite difference operator molecules according to equations (6), (7), and (8) respectively. Determination of these stresses is obtained by utilizing the iterated stress function values. The computer program for determining these stresses for the circular notch is shown in Appendix A.

After the stresses σ_x, σ_y, and τ_{xy} are computed, the principal stresses and their directions are determined. The governing equations are:[15]

$$\sigma_1 = \frac{\sigma_x + \sigma_y}{2} + \sqrt{\left(\frac{\sigma_x - \sigma_y}{2}\right)^2 + \tau^2_{xy}} \tag{13}$$

$$\sigma_2 = \frac{\sigma_x + \sigma_y}{2} - \sqrt{\left(\frac{\sigma_x - \sigma_y}{2}\right)^2 + \tau^2_{xy}} \tag{14}$$

---

[15]Seibert Fairman and Chester S. Cutshall, Mechanics of Materials, John Wiley and Sons, Inc., New York, 1953, p. 342.

and

$$\tan 2\theta = \frac{-2\tau_{xy}}{\sigma_x - \sigma_y} \qquad (15)$$

where

σ_1 = the major principal stress

σ_2 = the minor principal stress

and

θ = the angular orientation of the principal stresses with respect to the X-axis.

CHAPTER IV

PLATE PROBLEMS INVESTIGATED

A. Square Plate with Elliptical Cutout

To apply the theory previously presented a square plate with a centrally located elliptical notch is investigated. The plate is assumed to be perfectly elastic, homogeneous, and of uniform thickness. Also, it is assumed that the plate is perfectly flat before loading is applied, and that the loading is applied in the plane of the middle surface of the plate. The square plate is uniformly compressed along two opposite edges, while the other two edges are free. The length of each side of the plate is assumed to be 40 units and is subdivided into 40 nodal spacings. The value of the nodal spacing "h" is taken as unity to simplify mathematical calculations. The elliptical cutout at the center of the plate has a major diameter equal to one-half the width of the plate and a minor diameter equal to three-tenths the width of the plate. Thus the size of the plate is equal to 40h X 40h, while the size of the cutout is equal to 20h X 12h. This elliptical cutout is so oriented that its major axis is parallel to the sides of the plate under loading. The value of the uniform compression acting on the plate is taken as 20 units for convenience

and ease of mathematical calculations. However, the final results for the stresses in the plate are normalized to give relative results at different points.

As explained previously, only one quarter of the plate is considered for obtaining a solution for the boundary values of the stress function. Such a consideration allows the same number of nodal points dictated by the storage capacity of the computer to be distributed over a small area, thereby increasing the accuracy of the solution. However, the stress function equations derived by the finite difference technique shown in Chapter II apply only to boundaries with straight edges. Therefore it becomes essential to represent the elliptical shape of the notch with a series of straight lines to approximate the configuration of the elliptical shape. This approximation, as shown in Figure 4, follows as closely as possible the configuration of the notch. It is assumed that the mesh spacing is small enough not to introduce a significant error in the final results.

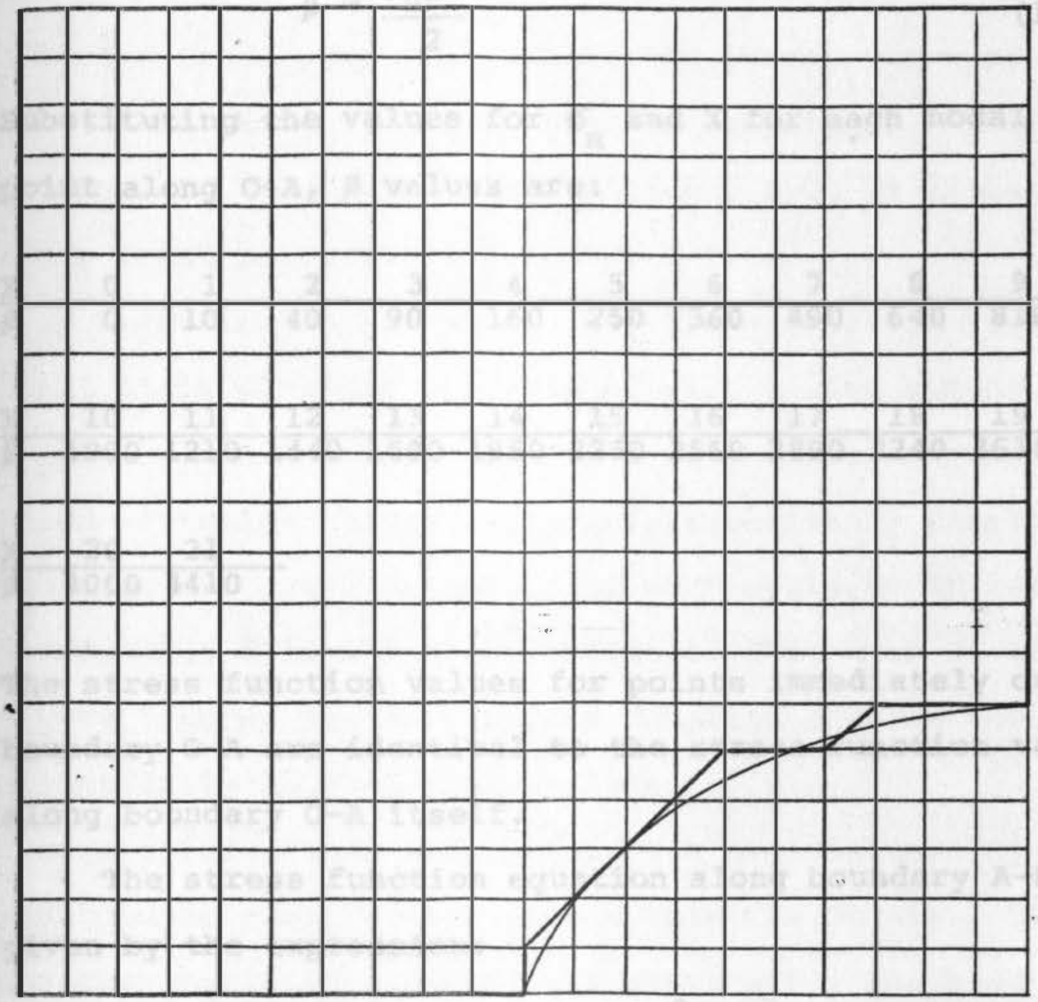

Figure 4. Elliptical Cutout Representation

The stress function equation along boundary O-A is given by the expression:

$$\emptyset = \frac{\sigma_n X^2}{2} \qquad (10\text{-a})$$

Substituting the values for σ_n and X for each nodal point along O-A, $\emptyset$ values are:

X	0	1	2	3	4	5	6	7	8	9
$\emptyset$	0	10	40	90	160	250	360	490	640	810

X	10	11	12	13	14	15	16	17	18	19
$\emptyset$	1000	1210	1440	1690	1960	2250	2560	2890	3240	3610

X	20	21
$\emptyset$	4000	4410

The stress function values for points immediately outside boundary O-A are identical to the stress function values along boundary O-A itself.

The stress function equation along boundary A-B is given by the expression:

$$\emptyset = \text{constant} = \frac{\sigma_n L^2}{2} \qquad (11\text{-a})$$

Substituting the values of σ_n and L, therefore:

$$\emptyset = \text{constant} = 4000$$

Each nodal point along boundary A-B is assigned this value.

The stress function values along boundaries B-C and D-O are determined by utilizing the iteration process and the symmetry conditions along these boundaries. Boundary C-D is a free edge. Therefore, the stress function values along this boundary are of constant magnitude. This value, as obtained at point C along boundary B-C, is assigned to every nodal point along boundary C-D.

Referring to Figure 3, the stress function value at point A' is obtained by extrapolation of the second degree parabola for the stress function along boundary O-A. Stress function values for points immediately outside boundary A-B are obtained after each cycle of iteration, by assuming a linear distribution of Ø between A' and B'. Figure 5 shows boundary stress function surface for the elliptically notched square plate.

Initial stress function values are arbitrarily assigned to every nodal point within the domain. Throughout the iteration process, the arbitrarily assigned stress function values are replaced each time by a modified computed value. As the convergence of the system continues, the biharmonic operator molecule becomes more nearly satisfied at each nodal point and the residual for each point iterated approaches zero. The computer program for computing the stress function value is shown in Appendix A, and the computed values themselves are shown

in Appendix B (Figure 16). Figure 6 shows the stress function contours obtained for this plate.

Knowing the stress function values at the different nodal points within and immediately beyond the domain, elastic stresses are determined for each nodal point according to equations 6, 7, 8, 13, 14, and 15. The computer programs to obtain such stresses are given in Appendix A. Figures 7, 8, and 9 show the contours obtained for σ_x, σ_y, and σ_{p_1} respectively, while the actual computed values for these quantities at each nodal point are shown in Appendix B (Figures 17, 18, and 20). Appendix B also shows the computer results for τ_{xy}, σ_{p_2}, and θ (Figures 19, 21, and 22).

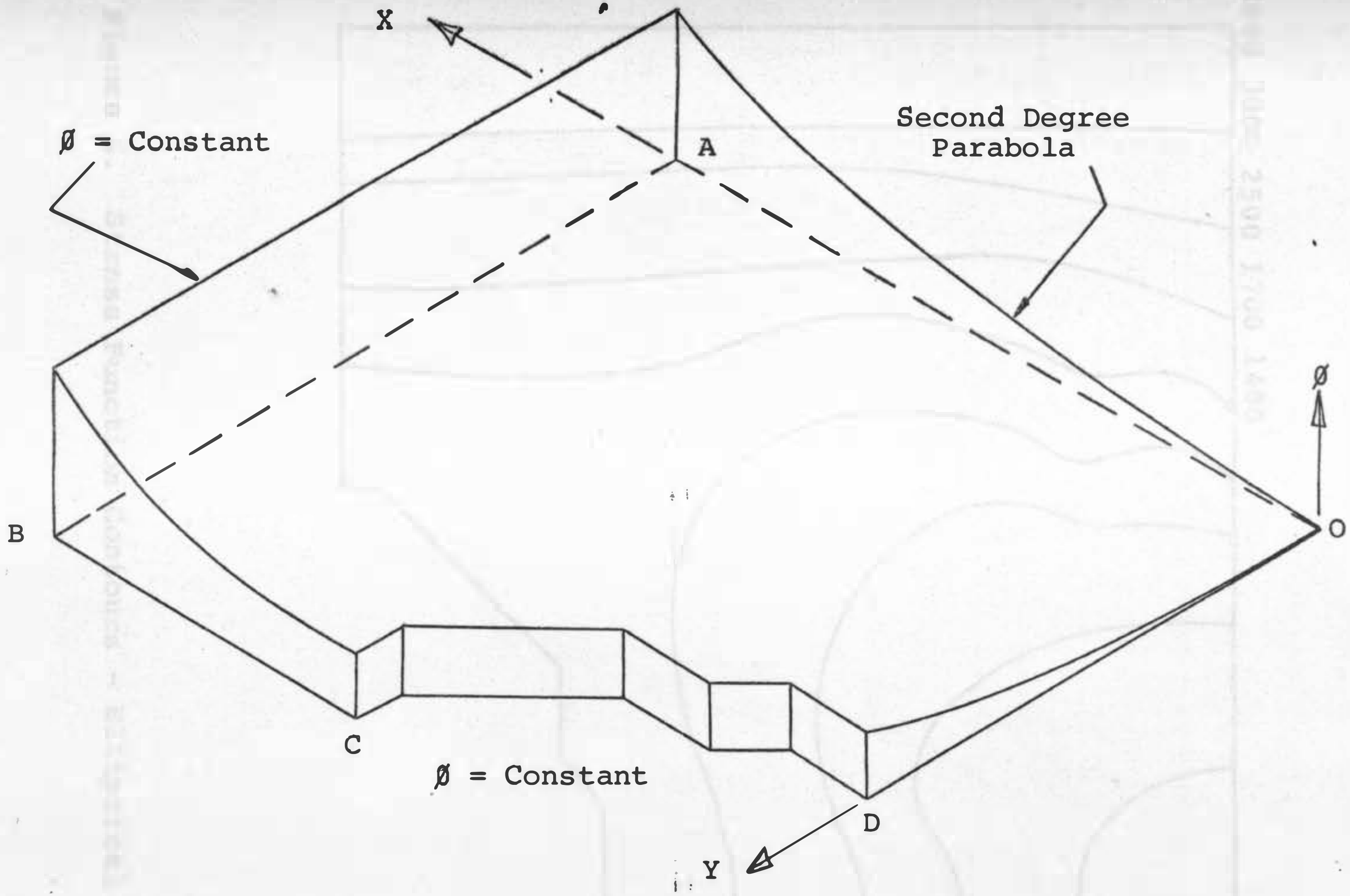

Figure 5. Stress Function Boundary Surface - Elliptical Cutout

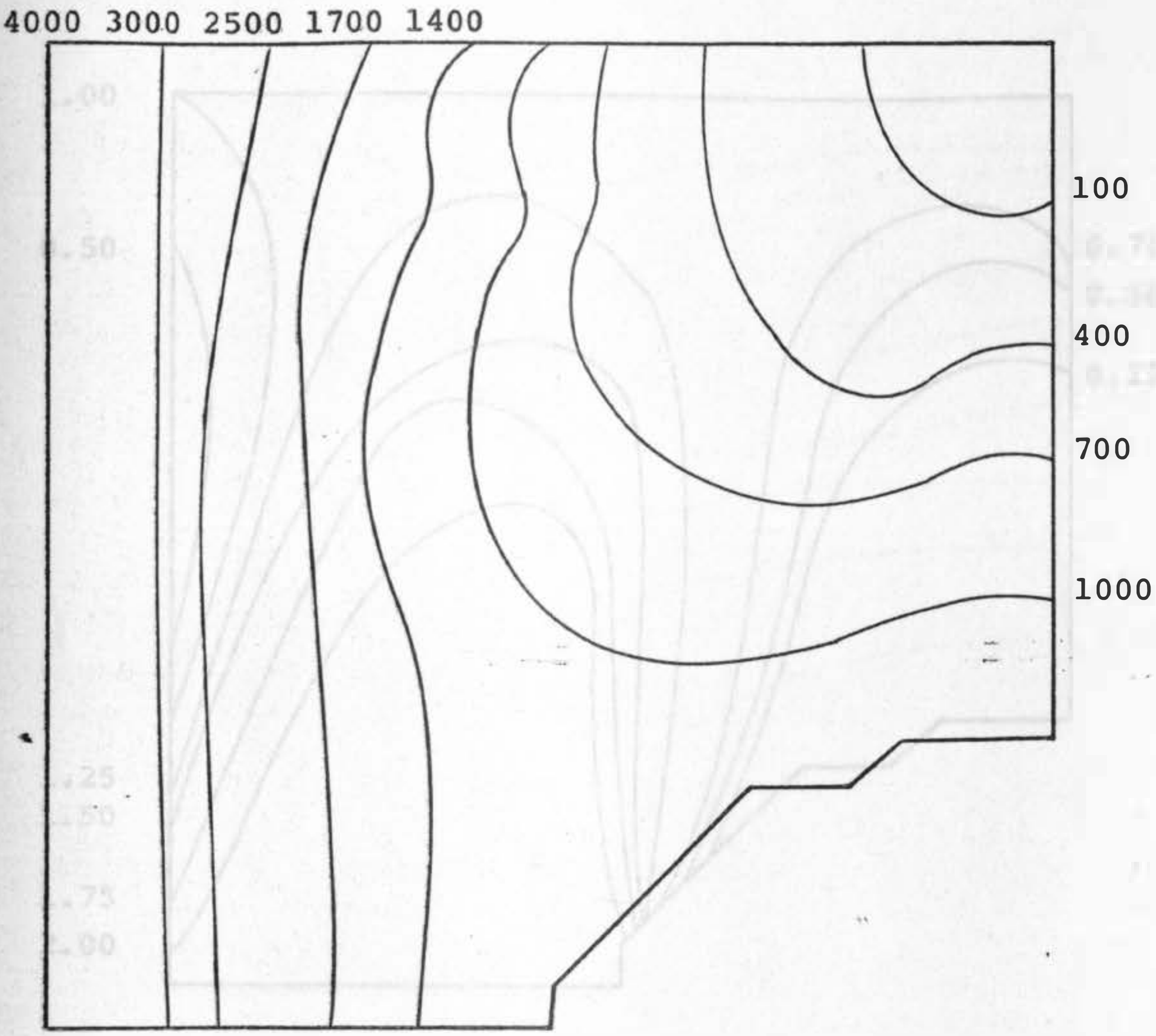

Figure 6. Stress Function Contours - Elliptical Cutout

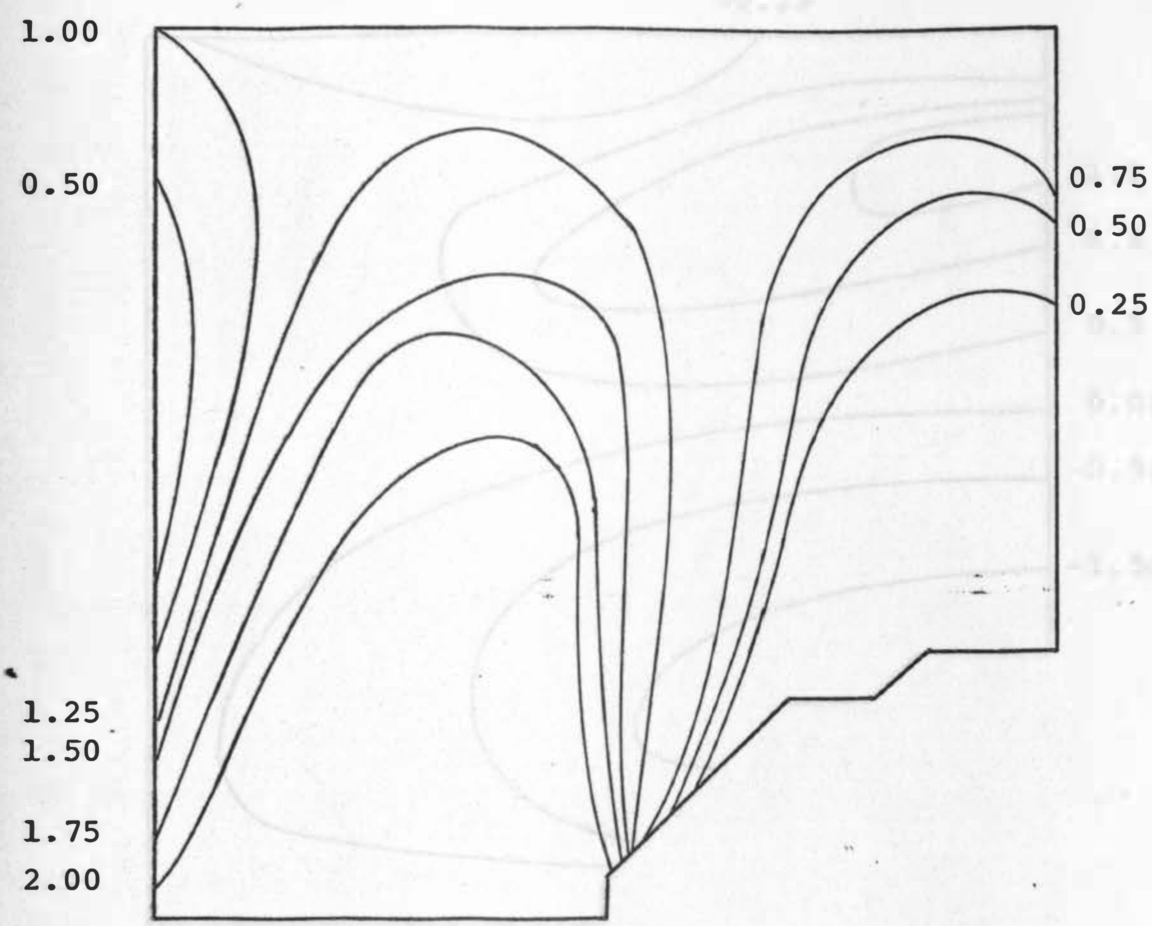

Figure 7. σ_x Contours - Elliptical Cutout

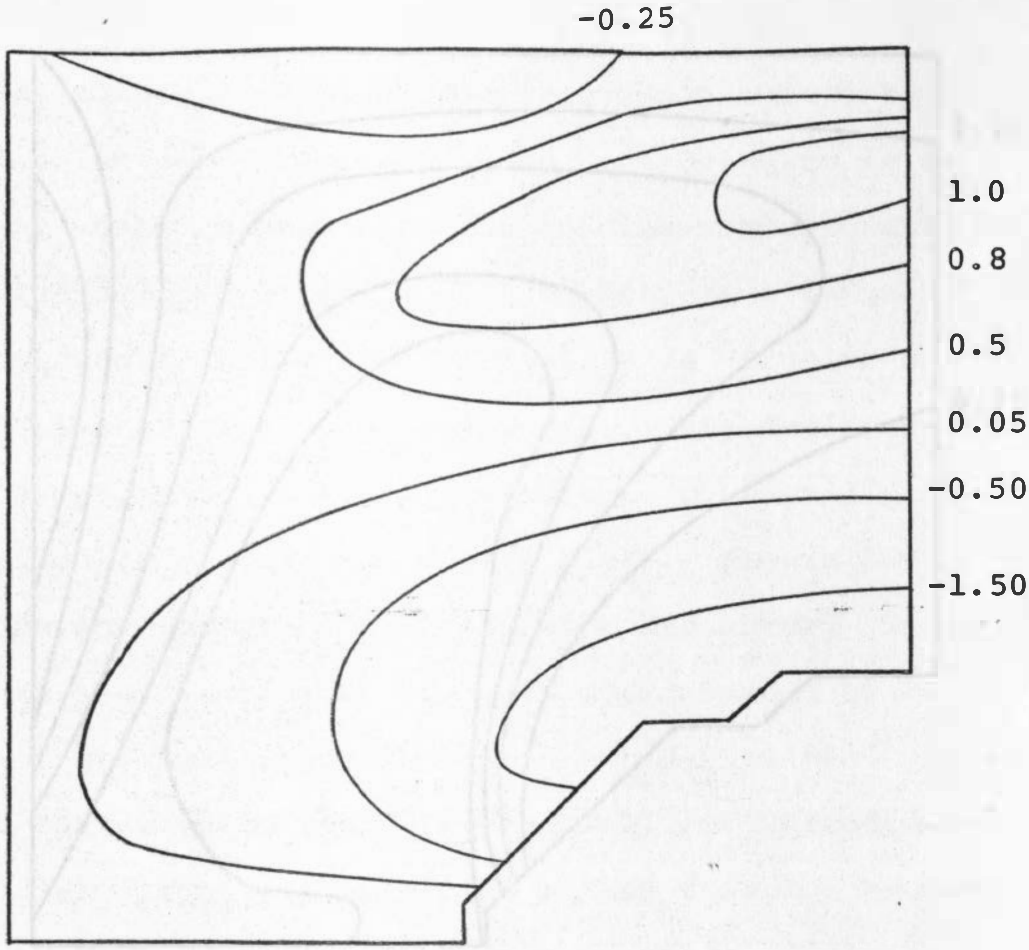

Figure 8. σ_y Contours - Elliptical Cutout

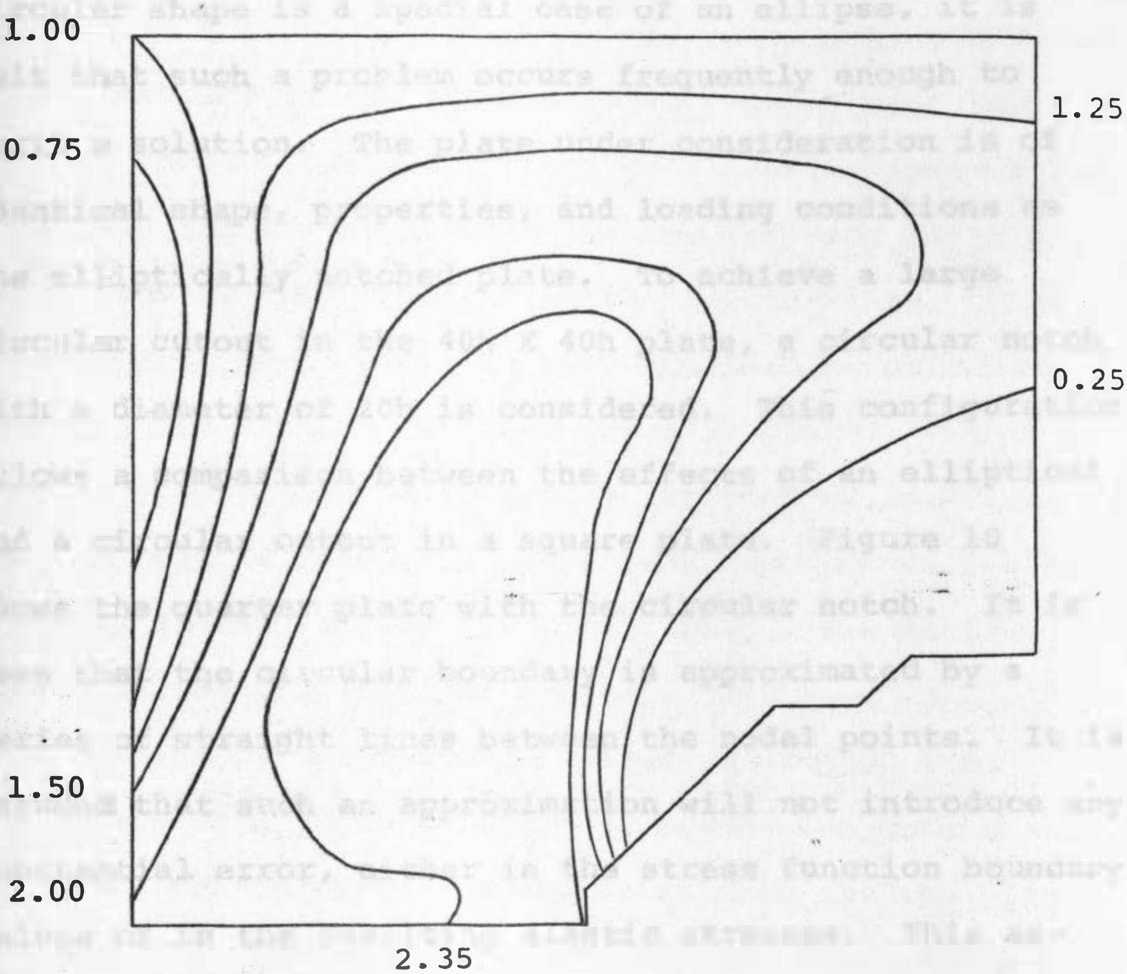

Figure 9. σ_{p_1} Contours - Elliptical Cutout

B. Square Plate with Circular Cutout

As a second example, the problem of a square plate with a circular cutout is also presented. Although a circular shape is a special case of an ellipse, it is felt that such a problem occurs frequently enough to merit a solution. The plate under consideration is of identical shape, properties, and loading conditions as the elliptically notched plate. To achieve a large circular cutout in the 40h X 40h plate, a circular notch with a diameter of 20h is considered. This configuration allows a comparison between the effects of an elliptical and a circular cutout in a square plate. Figure 10 shows the quarter plate with the circular notch. It is seen that the circular boundary is approximated by a series of straight lines between the nodal points. It is assumed that such an approximation will not introduce any substantial error, either in the stress function boundary values or in the resulting elastic stresses. This assumption is valid as long as the nodal spacing is small.

Utilizing the same plate and loading conditions as for the elliptically notched plate yields stress function values along boundaries O-A and A-B identical to those obtained for the elliptical cutout. Stress function values along boundaries B-C, C-D, and D-O as well as for points immediately outside the boundaries are determined

through similar procedures employed for the elliptically notched plate. Also, the stress function values within the domain are obtained through an iterative technique identical to the one utilized for the elliptically notched plate. Accuracy of the final results depends upon the degree of iteration. Therefore, the iterative process for determining the stress function values for each plate was made to consume approximately equal computer time. This utilization of equal computer time provided a valid comparison of the results obtained for each plate. Figure 11 shows the stress function boundary surface, while Figure 12 shows the contour lines for the stress function values for the square plate with the circular cutout. The actual computed values are shown in Appendix B (Figure 23).

After the stress function values at each of the nodal points within and immediately beyond the domain are determined, elastic stresses are calculated for the different points. The equations used are the same as the equations utilized for stress determination in the elliptically notched plate. Figures 13, 14, and 15 show the contours obtained for σ_x, σ_y, and σ_{p_1} respectively, while the actual computed values for these quantities at each nodal point are shown in Appendix B (Figures 24, 25, and 27). Computed values for τ_{xy}, σ_{p_2}, and θ for the

circularly notched plate are shown in Appendix B (Figures 26, 28, and 29).

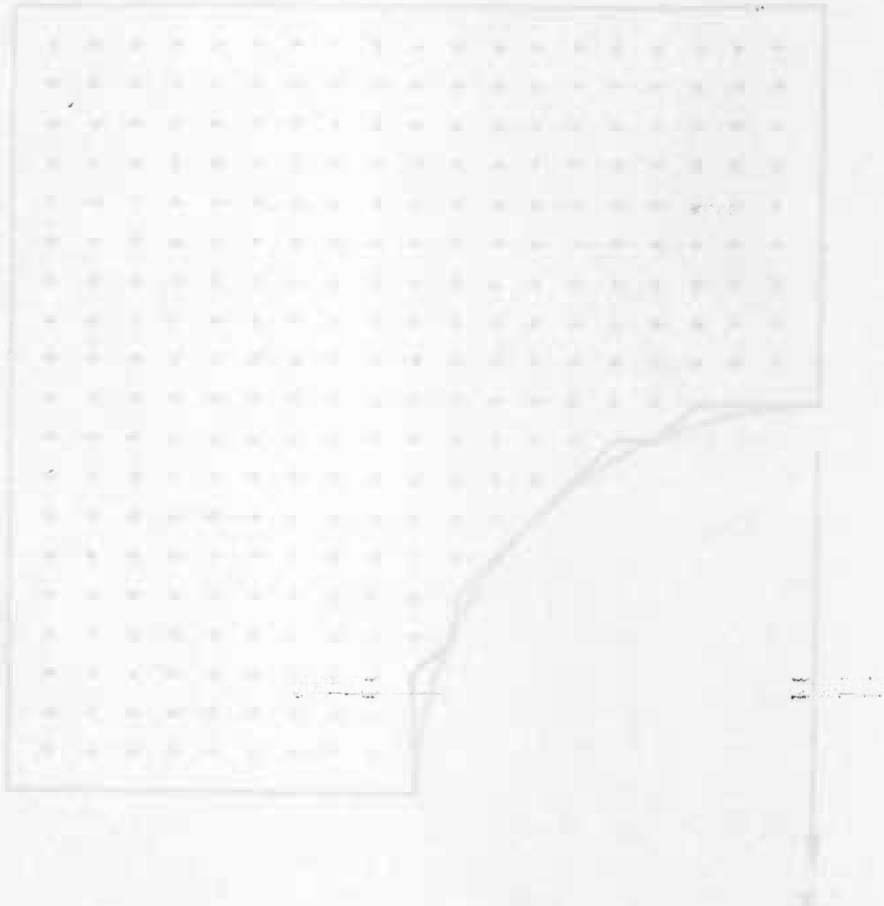

Figure 10. The Quarter Plate
Mesh Subdivision and Circular Notch Representation

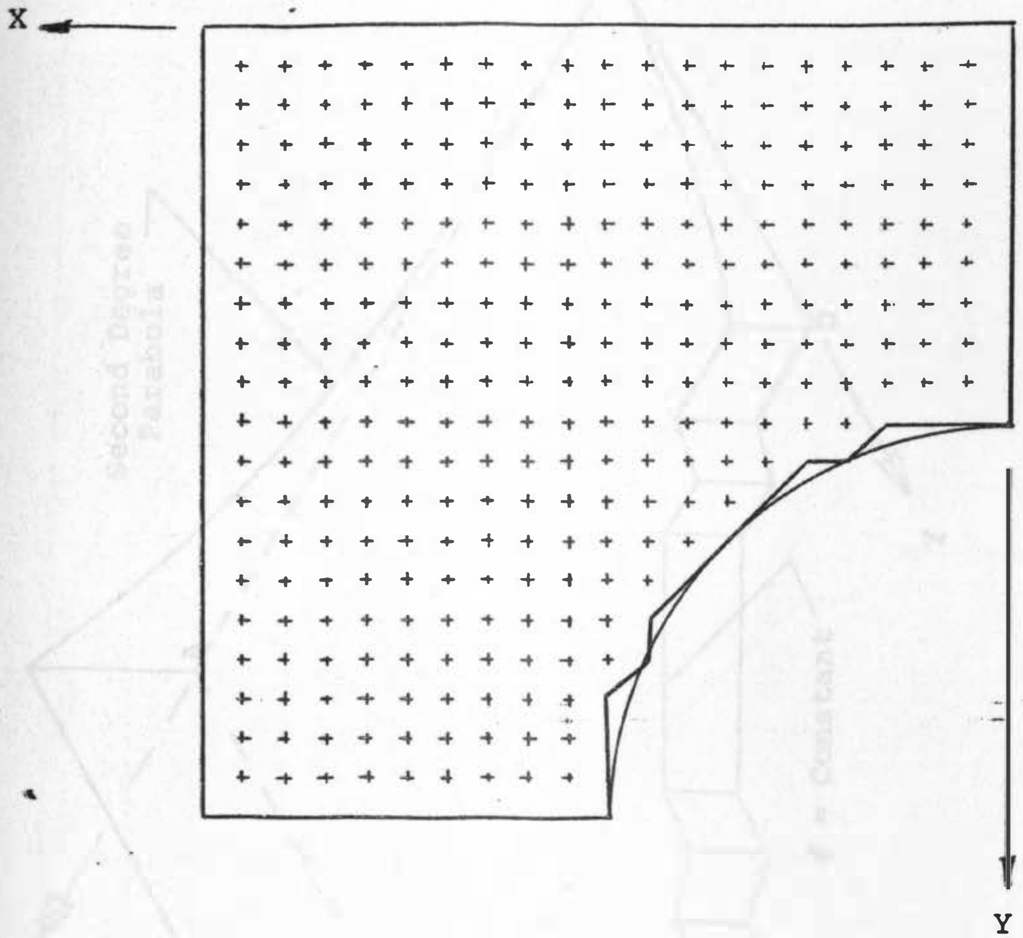

Figure 10. The Quarter Plate
Mesh Subdivision and Circular Notch Representation

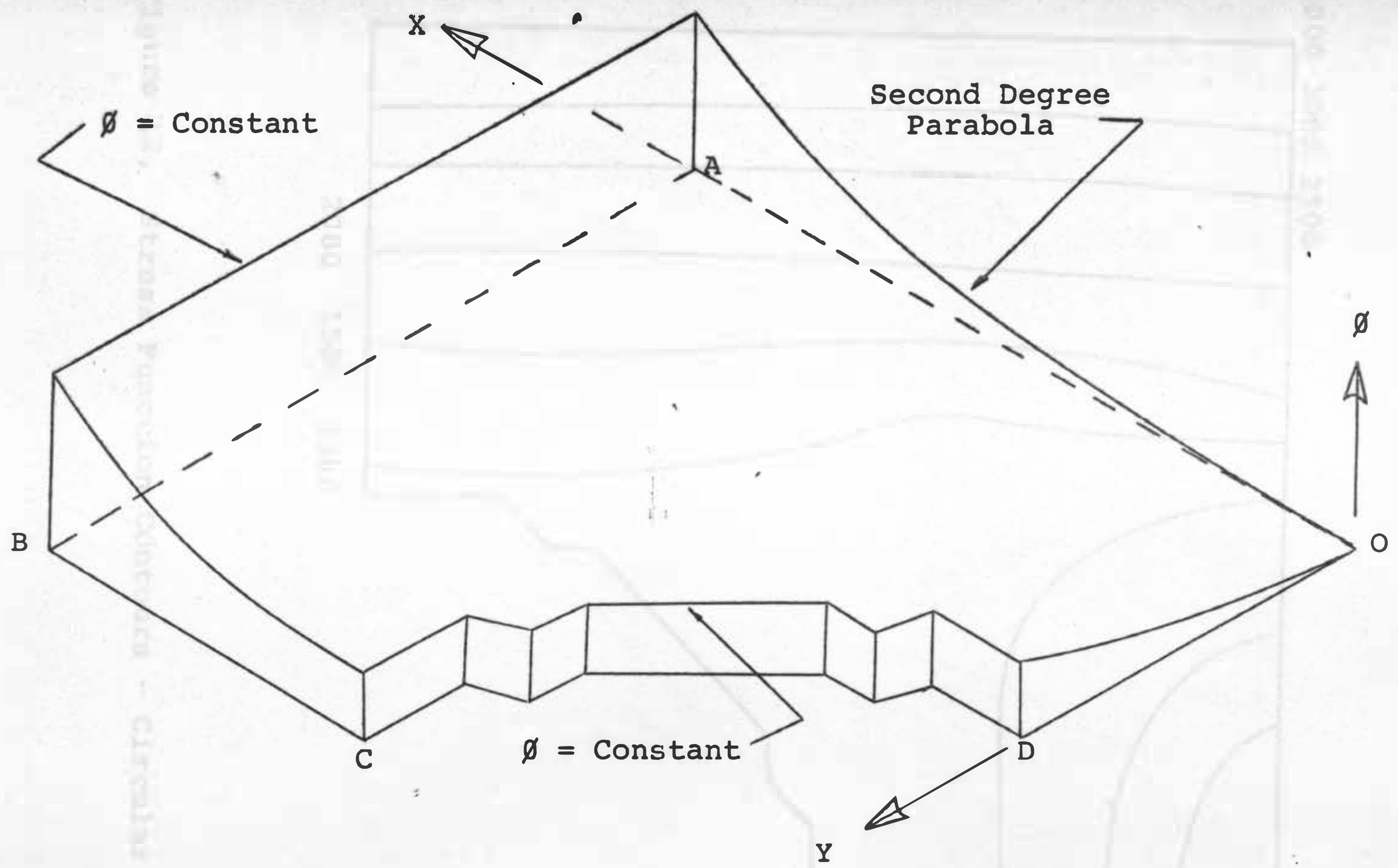

Figure 11. Stress Function Boundary Surface - Circular Cutout

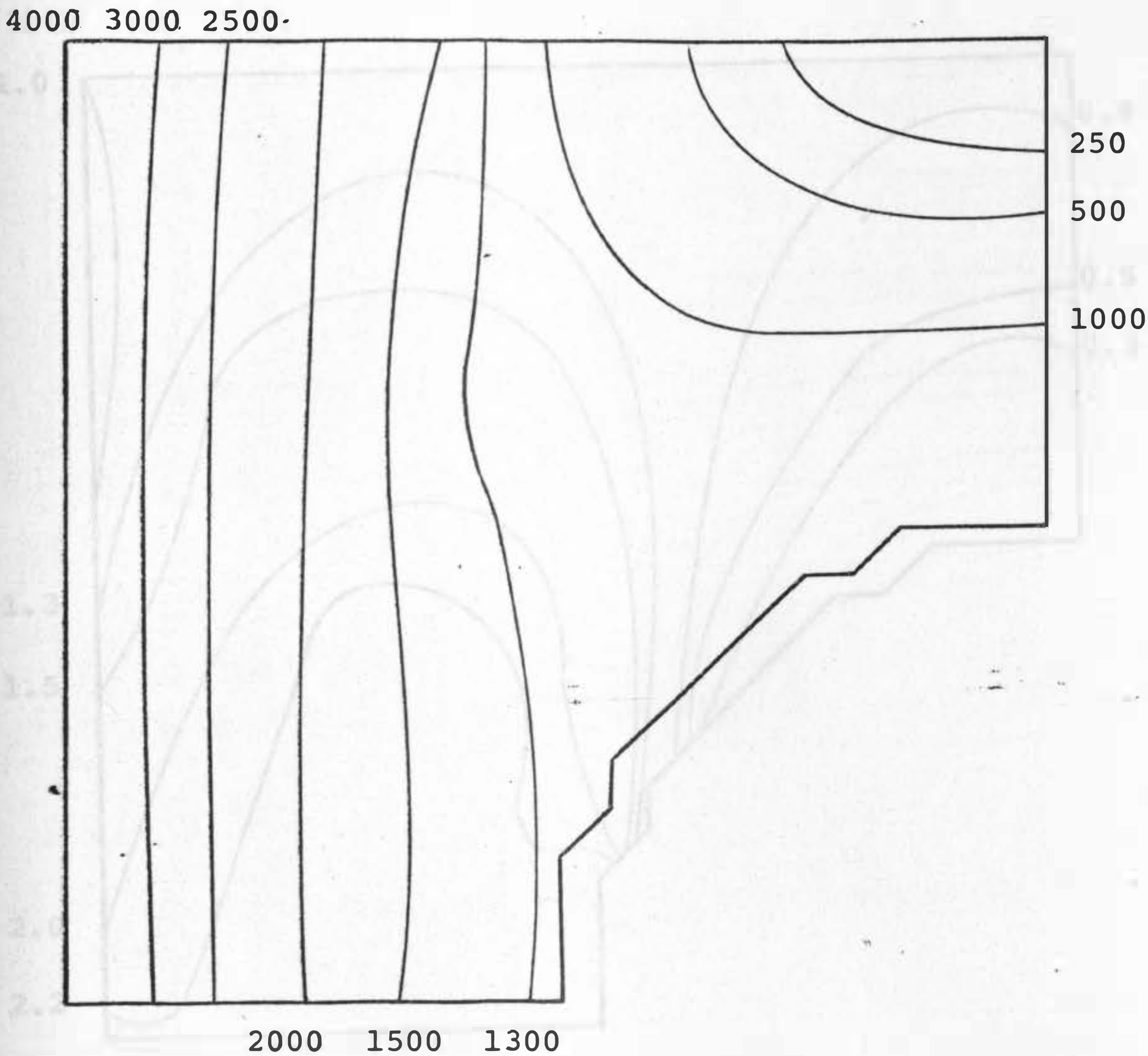

Figure 12. Stress Function Contours - Circular Cutout

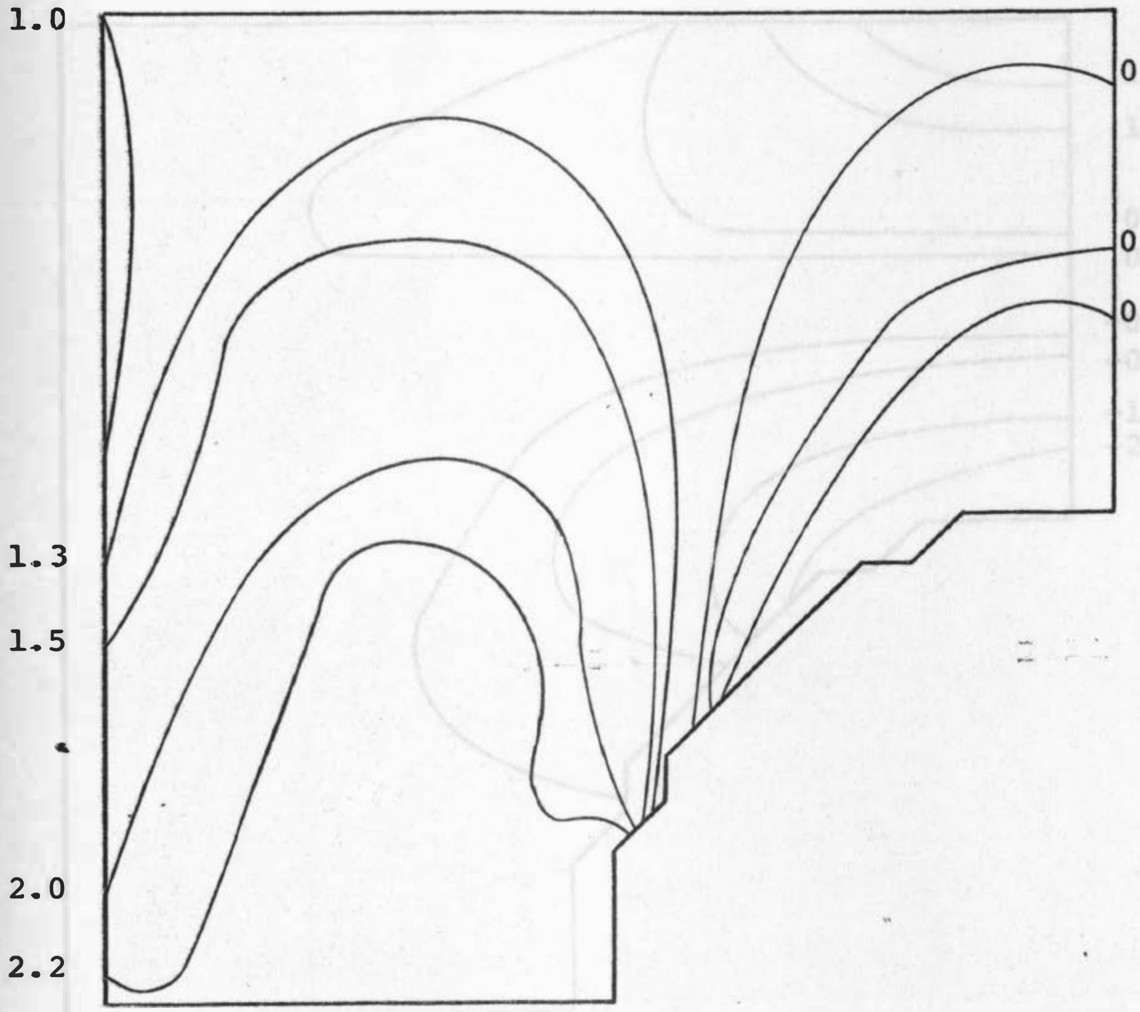

Figure 13. σ_x Contours - Circular Cutout

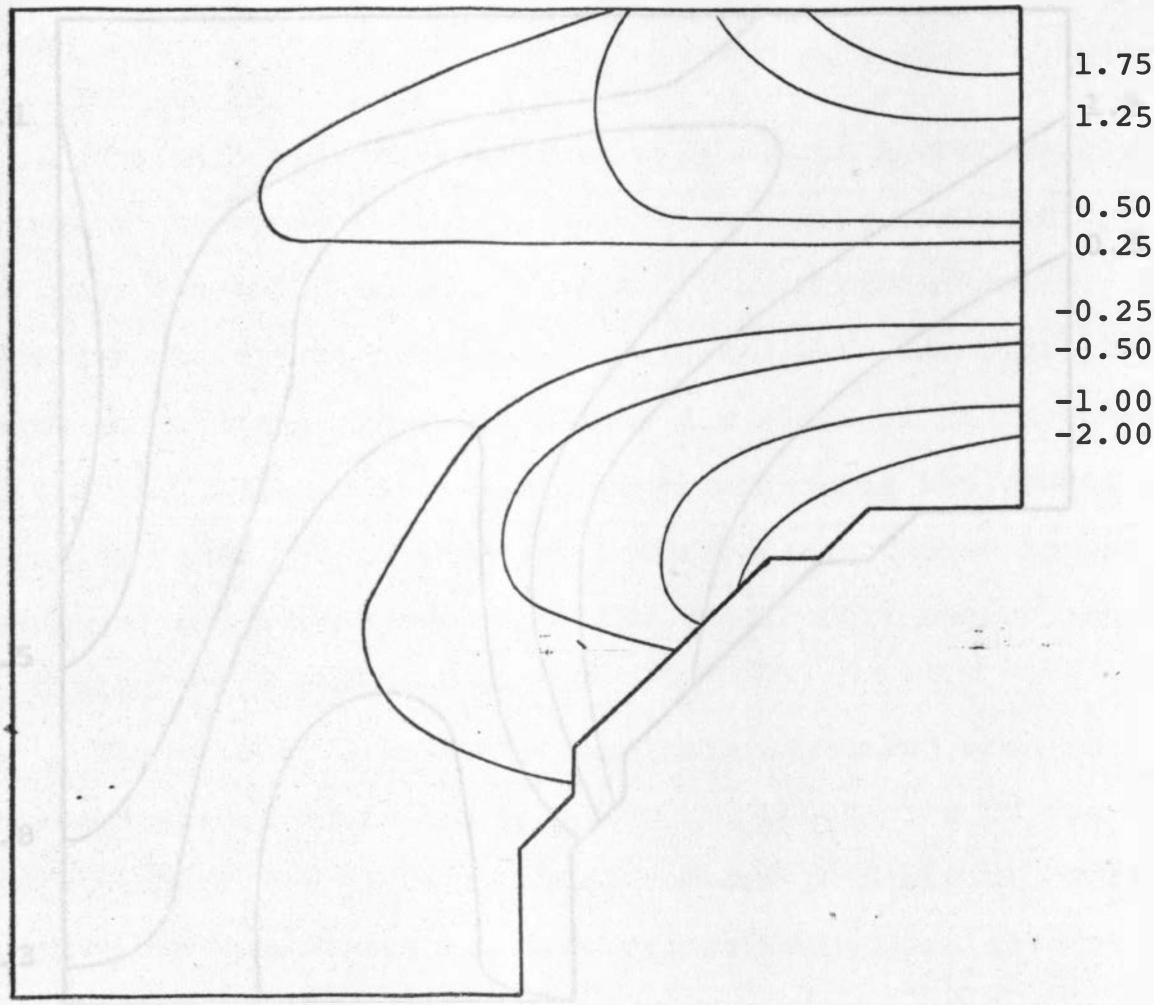

Figure 14. σ_y Contours - Circular Cutout

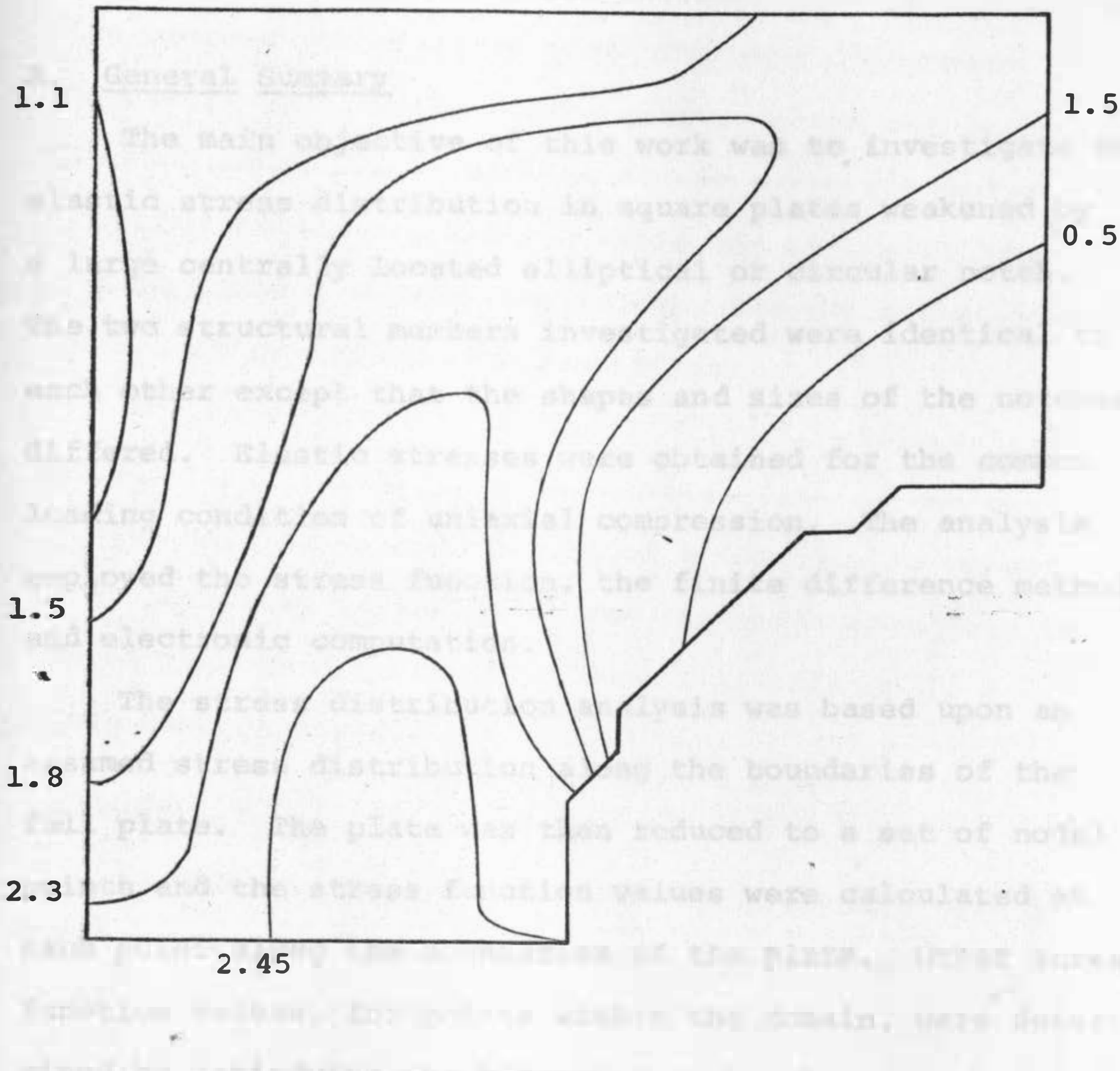

Figure 15. σ_{p_1} Contours - Circular Cutout

CHAPTER V

SUMMARY AND CONCLUSIONS

A. General Summary

The main objective of this work was to investigate the elastic stress distribution in square plates weakened by a large centrally located elliptical or circular notch. The two structural members investigated were identical to each other except that the shapes and sizes of the notches differed. Elastic stresses were obtained for the common loading condition of uniaxial compression. The analysis employed the stress function, the finite difference method, and electronic computation.

The stress distribution analysis was based upon an assumed stress distribution along the boundaries of the full plate. The plate was then reduced to a set of nodal points and the stress function values were calculated at each point along the boundaries of the plate. Other stress function values, for points within the domain, were determined by satisfying the biharmonic molecule at each point. The plate stresses were then determined.

For full utilization of the computer core capacity and to obtain maximum accuracy in satisfying the biharmonic function, only one quarther of the plate was considered.

The cutout configuration was approximated by a series of straight lines. However, these lines produced corners that acted as points of singularity. Although the iteration process was employed along the axes of symmetry of the plate, equilibrium of the quarter plate was satisfied. The horizontal throat section of the plate yielded a uniform stress distribution, while the vertical throat section yielded a balancing moment, thereby satisfying the necessary equilibrium conditions.

The results obtained for the elastic stresses are satisfactory, considering the complexities of the problem treated and the unavailability of a solution in closed form. Accuracy in the final results would have been improved if more computer time were available or if a finer mesh were used.

B. Conclusions

An analysis was presented of the procedure used in a digital program for computing the elastic stresses in square plates weakened by a centrally located large elliptical or circular notch. The theoretical basis of the procedure was outlined, and examples were presented of solutions computed by the program. This investigation has provided a quantitative theoretical evaluation of the elastic stresses in such plates.

The following conclusions may be drawn:

1. This work is considered as a basis for the solution of the eigenvalue problem for the plates investigated. It is possible to incorporate the determined elastic stresses into an eigenvalue problem and thereby to obtain the critical buckling coefficients for these plates.
2. The stress contours indicate that the corners produced by the series of lines approximating the elliptical or circular notch act as points of singularity, and thus introduce some error. Accuracy would have been improved by employing a modified biharmonic molecule. However, the amount of error introduced by such approximations is not significant. Moreover, lack of sufficient computer time and computer core capacity prohibited an extensive modification of the basic biharmonic molecule.
3. Comparing the stress contours for both plates indicates consistency in the results obtained for the elastic stress distribution. Nevertheless, the circular cutout produced higher stress concentration at both throat sections of the plate. This fact indicates that, for serving the same purpose, an elliptical cutout is more advantageous in structural engineering.

4. The computer time required for the iteration process was relatively long. This time can be reduced either by considering a lesser degree of accuracy, or by employing modified numerical techniques such as the finite element method.[16]
5. The results of this study showed that equilibrium conditions were satisfied for the quarter plate. The horizontal throat section of the plate yielded a uniform stress distribution, while the vertical throat section yielded a balancing moment. These results indicate that the assumptions made to obtain the stress function values along and immediately outside the boundaries are valid.
6. The error introduced by employing the finite difference technique in computing the elastic stresses is estimated to vary between eight and twelve per cent. Part of this error was caused by the inherent properties of finite differences approximations as well as the degree of iterative convergence.

---

[16] P. Paramasivam and J.K. Sridhar Rao, "Buckling of Plates of Abruptly Varying Stiffness," <u>Proceedings</u>, American Society of Civil Engineers, Structural Division, No. St6, Vol. 95 (June, 1969).

C. Future Areas of Study

The use of electronic computations and numerical techniques in structural engineering on such a wide scale is relatively new. There are many engineering problems that can be worked out utilizing such techniques. Some of the future areas of research are listed below.

1. This study was limited to elliptically or circularly notched square plates. Other types of notches can be studied. Such studies will lead to the determination of the most efficient type of notches that can be used in a structural member.
2. The critical buckling load for a structural member is always of great value to the structural engineer. An elastic stress distribution is a necessary first step for determining such critical loads. Since the elastic stress distribution is already computed, it is highly recommended that this investigation be expanded to include the determination of the buckling loads for the plates studied.
3. It has been shown that the stress function values immediately beyond the boundaries of the plate are of great importance. However, the published information for their accurate extrapolation is somewhat lacking. It is felt that a study in this area is valuable.

4. This study was limited to uniaxial compressive load applied to two opposite edges of a simply supported notched plate. The effect of different types of loads and supports needs further investigation.
5. A running check on the analytical results obtained in this study could be made by a photoelastic technique.

BIBLIOGRAPHY

1. Chow, L., H.D. Conway, and G. Winter, "Stress in Deep Beams," Transactions, American Society of Civil Engineers, Vol. 118, 1963.

2. Conway, H.D., L. Chow, and G.W. Morgan, "Analysis of Deep Beams," Journal of Applied Mechanics, Vol. 18, 1951.

3. Crandall, S.H., Engineering Analysis, McGraw-Hill Book Company, Incorporated, New York, 1956.

4. Fairman, S., and Chester S. Cutshall, Mechanics of Materials, John Wiley and Sons, Incorporated, New York, 1953.

5. Geer, F., "Stresses in Deep Beams," Journal of the American Concrete Institute, Vol. 56, 1960.

6. Hoffman, P., "Elastic Stress Distribution in Rectangularly Notched Members," Master of Science Thesis, South Dakota State University, Brookings, South Dakota, 1965.

7. Kanan, M., "Elastic Stress Distribution in and Stability of Rectangularly Notched Plates Axially Loaded by Uniform Compression," Master of Science Thesis, South Dakota State University, Brookings, South Dakota, 1967.

8. Paramasivam, P., and J.K. Sridhar Rao, "Buckling of Plates of Abruptly Varying Stiffness," Proceedings, American Society of Civil Engineers, Structural Division, No. St6, Vol. 95, 1969.

9. Shoukry, Z., "Elastic Flexural Stress Distribution in Webs of Castellated Steel Beams," Welding Journal, American Welding Society, Vol. 64, 1965.

10. Timoshenko, S., and J.H. Goodier, Theory of Elasticity, McGraw-Hill Book Company, Incorporated, New York, 1951.

11. Timoshenko, S., and S. Woinowsky-Krieger, Theory of Plates and Shells, Second Edition, McGraw-Hill Book Company, Incorporated, New York, 1961.

12. Turner, C.E., Introduction to Plate and Shell Theory, American Elsevier Publishing Company, Inc., New York, 1965.

13. Wang, P.C., Numerical and Matrix Methods in Structural Mechanics, John Wiley and Sons, Incorporated, New York, 1966.

14. White, R.N., and W.S. Cottingham, "Stability of Plates Under Partial Edge Loading," Proceedings, American Society of Civil Engineers, Engineering Mechanics Division, Vol. 88, No. 3297, 1962.

15. Zienkiewics, O.C., and G.S. Hollister, Stress Analysis, John Wiley and Sons, Limited, London, 1965.

APPENDIX A

COMPUTER PROGRAMS

```
C     A FORTRAN IV PROGRAM FOR SATISFYING THE BIHARMONIC
C     MOLECULE AS APPLIED TO A SQUARE PLATE WITH AN ELLIPTICAL NOTCH
C     PLATE SIZE 40X40
C     NOTCH SIZE 6 X 10
C     AXIAL UNIFORMLY DISTRIBUTED COMPRESSION APPLIED.
      DIMENSION F(24,24)
      CALL SWITCH(ISW)
      ISW=0
    3 FORMAT(10F7.0/10F7.0/4F7.0)
    4 FORMAT(F10.4,F10.4)
    5 FORMAT(10F7.0/10F7.0/4F7.0)
    9 FORMAT(24F5.0)
C     CLEAR THE ARRAYS
    6 DO 7 I=1,24
      DO 7 J=1,24
    7 F(I,J)=0.0
    8 READ (11,3) ((F(I,J),J=1,24),I=1,24)
  110 CONTINUE
   12 TEST = 0.0
      DCT = 0.0
      DO 29 I=3,22
      DO 29 J=3,15
   15 ELEM=(8.*(F(I&1,J)&F(I,J&1)&F(I-1,J)&F(I,J-1))
     C-2.*(F(I&1,J&1)&F(I&1,J-1)&F(I-1,J&1)&F(I-1,J-1))
     C-1.*(F(I,J&2)&F(I&2,J)&F(I,J-2)&F(I-2,J)))/20.
      ECK=ABS(F(I,J)-ELEM)
      IF (ECK-TEST)25,23,23
   23 TEST=ECK
   25 DECK=ABS(ECK/ELEM)
      IF (DECK-DCT)29,27,27
   27 DCT=DECK
   29 F(I,J)=ELEM
```

```
1000 DO 1001 J=1,17
1001 F(23,J)=F(21,J)
1002 DO 1003 J=1,17
1003 F(24,J)=F(20,J)
 520 F(22,1)=3.*(F(22,2)-F(22,3))&F(22,4)
 511 J=1
     DO 521 I=3,21
 521 F(I,J)=F(I-1,J)&((F(22,1)-F(2,1))/19.)
  33 DO 49 I=3,11
     DO 49 J=16,22
  35 ELEM=(8.*(F(I&1,J)&F(I,J&1)&F(I-1,J)&F(I,J-1))
    C-2.*(F(I&1,J&1)&F(I&1,J-1)&F(I-1,J&1)&F(I-1,J-1))
    C-1.*(F(I,J&2)&F(I&2,J)&F(I,J-2)&F(I-2,J)))/2 .
     ECK=ABS(F(I,J)-ELEM)
     IF(ECK-TEST)45,43,43
  43 TEST=ECK
  45 DECK=ABS(ECK/ELEM)
     IF (DECK-DCT)49,47,47
  47 DCT=DECK
  49 F(I,J)=ELEM
 400 DO 401 I=1,14
 401 F(I,23)=F(I,21)
 402 DO 403 I=1,14
 403 F(I,24)=F(I,20)
 500 J=16
     I=22
 501 ELEM=(8.*(F(I&1,J)&F(I,J&1)&F(I-1,J)&F(I,J-1))
    C-2.*(F(I&1,J&1)&F(I&1,J-1)&F(I-1,J&1)&F(I-1,J-1))
    C-1.*(F(I,J&2)&F(I&2,J)&F(I,J-2)&F(I-2,J)))/20.
 169 F(I,J)=ELEM
 510 B=F(22,16)
1004 J=16
```

```
      DO 1005 I=19,24
 1005 F(I,J)=B
 1012 J=17
      DO 1013 I=16,18
 1013 F(I,J)=B
 1014 F(15,18)=B
      F(14,19)=B
      F(13,20)=B
 1022 I=12
      DO 1023 J=21,23
 1023 F(I,J)=B
 1024 F(22,17)=3.*(F(22,16)-F(22,15))&F(22,14)
      C=F(22,17)
  512 I=22
      J=18
  513 F(I,J)=3.*(F(22,17)-F(22,16))&F(22,15)
 2004 J=17
      DO 2005 I=19,24
 2005 F(I,J)=C
 2006 J=18
      DO 2007 I=16,19
 2007 F(I,J)=C
      F(16,19)=C
      F(15,19)=C
      F(13,20)=C
 2008 I=14
      DO 2009 J=20,21
 2009 F(I,J)=C
 2010 I=13
      DO 2011 J=21,23
 2011 F(I,J)=C
   73 J=16
```

```
      DO 89 I=12,18
   75 ELEM=(8.*(F(I&1,J)&F(I,J&1)&F(I-1,J)&F(I,J-1))
     C-2.*(F(I&1,J&1)&F(I&1,J-1)&F(I-1,J&1)&F(I-1,J-1))
     C-1.*(F(I,J&2)&F(I&2,J)&F(I,J-2)&F(I-2,J)))/20.
      ECK=ABS(F(I,J)-ELEM)
      IF(ECK-TEST)85,83,83
   83 TEST=ECK
   85 DECK=ABS(ECK/ELEM)
      IF (DECK-DCT)89,87,87
   87 DCT=DECK
   89 F(I,J)=ELEM
   93 J=17
      DO 109 I=12,15
   95 ELEM=(8.*(F(I&1,J)&F(I,J&1)&F(I-1,J)&F(I,J-1))
     C-2.*(F(I&1,J&1)&F(I&1,J-1)&F(I-1,J&1)&F(I-1,J-1))
     C-1.*(F(I,J&2)&F(I&2,J)&F(I,J-2)&F(I-2,J)))/20.
      ECK=ABS(F(I,J)-ELEM)
      IF(ECK-TEST)105,103,103
  103 TEST=ECK
  105 DECK=ABS(ECK/ELEM)
      IF (DECK-DCT)109,107,107
  107 DCT=DECK
  109 F(I,J)=ELEM
  113 J=18
      DO 129 I=12,14
  115 ELEM=(8.*(F(I&1,J)&F(I,J&1)&F(I-1,J)&F(I,J-1))
     C-2.*(F(I&1,J&1)&F(I&1,J-1)&F(I-1,J&1)&F(I-1,J-1))
     C-1.*(F(I,J&2)&F(I&2,J)&F(I,J-2)&F(I-2,J)))/20.
      ECK=ABS(F(I,J)-ELEM)
      IF(ECK-TEST)125,123,123
  123 TEST=ECK
  125 DECK=ABS(ECK/ELEM)
```

```
129 F(I,J)=ELEM
800 J=19
    DO 149 I=12,13
155 ELEM=(8.*(F(I&1,J)&F(I,J&1)&F(I-1,J)&F(I,J-1))
   C-2.*(F(I&1,J&1)&F(I&1,J-1)&F(I-1,J&1)&F(I-1,J-1))
   C-1.*(F(I,J&2)&F(I&2,J)&F(I,J-2)&F(I-2,J)))/20.
    ECK=ABS(F(I,J)-ELEM)
    IF(ECK-TEST)145,143,143
143 TEST=ECK
145 DECK=ABS(ECK/ELEM)
    IF (DECK-DCT)149,147,147
147 DCT=DECK
149 F(I,J)=ELEM
133 I=12
    J=20
135 ELEM=(8.*(F(I&1,J)&F(I,J&1)&F(I-1,J)&F(I,J-1))
   C-2.*(F(I&1,J&1)&F(I&1,J-1)&F(I-1,J&1)&F(I-1,J-1))
   C-1.*(F(I,J&2)&F(I&2,J)&F(I,J-2)&F(I-2,J)))/20.
749 F(I,J)=ELEM
    WRITE  (12,4) TEST,DCT
    IF (ISW)110,110,74
 74 WRITE (13,5)((F(I,J),J=1,24),I=1,24)
700 WRITE(12,9)((F(I,J),J=1,24),I=1,24)
    STOP
    END
```

```
C       A FORTRAN IV FOR COMPUTING STRESSES AT NODAL POINTS OF A PLATE
C       WHOSE STRESS FUNCTION VALUES ARE DETERMINED)
      1 FORMAT (10F7.0/10F7.0/4F7.0)
      2 FORMAT (21F6.2)
      3 FORMAT (11F7.2/10F7.2)
        DIMENSION F(24,24)
        DIMENSION TXY(21,21)
        DIMENSION SIGX(21,21)
        DIMENSION SIGY(21,21)
C       CLEAR THE ARRAYS
      4 READ (11,1) ((F(I,J),J=1,24),I=1,24)
      5 DO 6 I=2,22
        DO 6  J=2,22
        SIGX(I,J)=0.0
        SIGY(I,J)=0.0
      6 TXY(I,J)=0.0
        DO 7 I=2,22
        DO 7 J=2,12
        SIGX(I,J)=(F(I,J&1)&F(I,J-1)-2.*F(I,J))/20.
        SIGY(I,J)=(F(I-1,J)&F(I&1,J)-2.*F(I,J))/20.
      7 TXY(I,J)=(F(I-1,J-1)&F(I&1,J&1)-F(I&1,J-1)
       C-F(I-1,J&1))/80.
        DO 8 I=2,16
        DO 8 J=13,22
        SIGX(I,J)=(F(I,J&1)&F(I,J-1)-2.*F(I,J))/20.
        SIGY(I,J)=(F(I-1,J)&F(I&1,J)-2.*F(I,J))/20.
      8 TXY(I,J)=(F(I-1,J-1)&F(I&1,J&1)-F(I&1,J-1)
       C-F(I-1,J&1))/80.
        I=17
        DO 9 J=13,18
        SIGX(I,J)=(F(I,J&1)&F(I,J-1)-2.*F(I,J))/20.
        SIGY(I,J)=(F(I-1,J)&F(I&1,J)-2.*F(I,J))/20.
```

```
  9 TXY(I,J)=(F(I-1,J-1)&F(I&1,J&1)-F(I&1,J-1)
   C-F(I-1,J&1))/80.
    I=18
    DO 10 J=13,15
    SIGX(I,J)=(F(I,J&1)&F(I,J-1)-2.*F(I,J))/20.
    SIGY(I,J)=(F(I-1,J)&F(I&1,J)-2.*F(I,J))/20.
 10 TXY(I,J)=(F(I-1,J-1)&F(I&1,J&1)-F(I&1,J-1)
   C-F(I-1,J&1))/80.
    I=19
    DO 11 J=13,14
    SIGX(I,J)=(F(I,J&1)&F(I,J-1)-2.*F(I,J))/20.
    SIGY(I,J)=(F(I-1,J)&F(I&1,J)-2.*F(I,J))/20.
 11 TXY(I,J)=(F(I-1,J-1)&F(I&1,J&1)-F(I&1,J-1)
   C-F(I-1,J&1))/80.
    I=20
    DO 12 J=13
    SIGX(I,J)=(F(I,J&1)&F(I,J-1)-2.*F(I,J))/20.
    SIGY(I,J)=(F(I-1,J)&F(I&1,J)-2.*F(I,J))/20.
 12 TXY(I,J)=(F(I-1,J-1)&F(I&1,J&1)-F(I&1,J-1)
   C-F(I-1,J&1))/80.
    J=2
    DO 13 I=2,22
 13 TXY(I,J)=0.0
100 FORMAT (1H1,40H THE FOLLOWING ARE ELEMENTS OF SIGX(I,J))
    WRITE (12,100)
    WRITE (12,2) ((SIGX(I,J),J=2,22),I=2,22)
    WRITE (13,100)
    WRITE (13,3) ((SIGX(I,J),J=2,22),I=2,22)
 35 FORMAT (1H1,40H THE FOLLOWING ARE ELEMENTS OF SIGY(I,J))
    WRITE (12,35)
    WRITE (12,2) ((SIGY(I,J),J=2,22),I=2,22)
    WRITE (13,35)
```

```
      WRITE (13,3) ((SIGY(I,J),J=2,22),I=2,22)
   55 FORMAT (1H1,39H THE FOLLOWING ARE ELEMENTS OF TXY(I,J))
      WRITE (12,55)
      WRITE(12,2) ((TXY(I,J),J=2,22),I=2,22)
      WRITE(13,3) ((TXY(I,J),J=2,22),I=2,22)
      STOP
      END
```

```
C       A FORTRAN IV PROGRAM FOR
C       COMPUTING PRINCIPAL STRESSES
    100 FORMAT (21F6.2)
      1 FORMAT (11F7.2/10F7.2)
        DIMENSION SIGX(21,21)
        DIMENSION SIGY(21,21)
        DIMENSION TXY(21,21)
        DIMENSION SIGP1(21,21)
        DIMENSION SIGP2(21,21)
        DIMENSION ANGL(21,21)
        DIMENSION BIG(21,21)
      2 READ (11,1) ((SIGX(I,J),J=1,21),I=1,21)
      3 READ (11,1) ((SIGY(I,J),J=1,21),I=1,21)
      4 READ (11,1) ((TXY(I,J),J=1,21),I=1,21)
      5 DO 6 I=1,21
        DO 6 J=1,21
        SIGP1(I,J)=0.0
        ANGL(I,J)=0.0
      6 SIGP2(I,J)=0.0
      7 DO 8 I=1,21
        DO 8 J=1,11
        D=SQRT(((SIGX(I,J)-SIGY(I,J))/2.)**2&TXY(I,J)**2)
        SP=(SIGX(I,J)&SIGY(I,J))/2.
        SIGP1(I,J)=SP&D
        SIGP2(I,J)=SP-D
      8 ANGL(I,J)=ATAN(-TXY(I,J)*2./(SIGX(I,J)
       C-SIGY(I,J)))*28.648
      9 DO 10 I=1,15
        DO 10 J=12,21
        D=SQRT(((SIGX(I,J)-SIGY(I,J))/2.)**2&TXY(I,J)**2)
        SP=(SIGX(I,J)&SIGY(I,J))/2.
        SIGP1(I,J)=SP&D
```

```
      SIGP2(I,J)=SP-D
   10 ANGL(I,J)=ATAN(-TXY(I,J)*2./(SIGX(I,J)
     C-SIGY(I,J)))*28.648
   11 I=17
      DO 12 J=12,14
      D=SQRT(((SIGX(I,J)-SIGY(I,J))/2.)**2&TXY(I,J)**2)
      SP=(SIGX(I,J)&SIGY(I,J))/2.
      SIGP1(I,J)=SP&D
      SIGP2(I,J)=SP-D
   12 ANGL(I,J)=ATAN(-TXY(I,J)*2./(SIGX(I,J)
     C-SIGY(I,J)))*28.648
   13 I=18
      DO 14 J=12,13
      D=SQRT(((SIGX(I,J)-SIGY(I,J))/2.)**2&TXY(I,J)**2)
      SP=(SIGX(I,J)&SIGY(I,J))/2.
      SIGP1(I,J)=SP&D
      SIGP2(I,J)=SP-D
   14 ANGL(I,J)=ATAN(-TXY(I,J)*2./(SIGX(I,J)
     C-SIGY(I,J)))*28.648
   15 I=19
      DO 16 J=12
      D=SQRT(((SIGX(I,J)-SIGY(I,J))/2.)**2&TXY(I,J)**2)
      SP=(SIGX(I,J)&SIGY(I,J))/2.
      SIGP1(I,J)=SP&D
      SIGP2(I,J)=SP-D
   16 ANGL(I,J)=ATAN(-TXY(I,J)*2./(SIGX(I,J)
     C-SIGY(I,J)))*28.648
   27 FORMAT (1H1,40H THE FOLLOWING ARE ELEMENTS OF ANGL(I,J))
   28 FORMAT (1H1,41H THE FOLLOWING ARE ELEMENTS OF SIGP2(I,J))
   30 FORMAT (1H1,41H THE FOLLOWING ARE ELEMENTS OF SIGP1(I,J))
      WRITE (12,27)
      WRITE (12,100) ((ANGL(I,J),J=1,21),I=1,21)
```

```
WRITE (13,27)
WRITE (13,1) ((ANGL(I,J),J=1,21),I=1,21)
WRITE (12,30)
WRITE (12,100) ((SIGP1(I,J),J=1,21),I=1,21)
WRITE (13,30)
WRITE (13,1) ((SIGP1(I,J),J=1,21),I=1,21)
WRITE(12,28)
WRITE (12,100) ((SIGP2(I,J),J=1,21),I=1,21)
WRITE(13,28)
WRITE (13,1) ((SIGP2(I,J),J=1,21),I=1,21)
STOP
END
```

APPENDIX B

ELASTIC STRESSES COMPUTER OUTPUT

4410.	4000.	3610.	3240.	2890.	2560.	2250.	1960.	1690.	1440.	1210.	1000.	810.	640.	490.	360.	250.	160.	90.	40.	10.	0.	10.	4
4410.	4000.	3610.	3240.	2890.	2560.	2250.	1960.	1690.	1440.	1210.	1000.	810.	640.	490.	360.	250.	160.	90.	40.	10.	0.	10.	4
4416.	4000.	3605.	3229.	2873.	2536.	2223.	1930.	1658.	1408.	1179.	972.	787.	622.	478.	354.	249.	163.	96.	47.	18.	8.	18.	4
4422.	4000.	3596.	3211.	2846.	2502.	2180.	1881.	1607.	1357.	1131.	929.	751.	595.	461.	347.	251.	173.	112.	66.	35.	24.	35.	6
4428.	4000.	3587.	3190.	2813.	2458.	2128.	1824.	1547.	1297.	1076.	881.	712.	568.	446.	345.	262.	195.	141.	100.	71.	56.	71.	10
4434.	4000.	3576.	3157.	2778.	2413.	2074.	1764.	1486.	1238.	1022.	836.	678.	548.	441.	355.	286.	232.	190.	159.	138.	130.	138.	15
4440.	4000.	3566.	3146.	2745.	2370.	2024.	1710.	1430.	1186.	976.	800.	656.	540.	449.	379.	326.	287.	259.	238.	224.	218.	224.	23
4446.	4000.	3557.	3126.	2716.	2332.	1981.	1664.	1386.	1146.	944.	779.	648.	548.	474.	421.	385.	361.	346.	337.	332.	329.	332.	33
4452.	4000.	3549.	3110.	2692.	2303.	1947.	1631.	1355.	1122.	929.	776.	660.	575.	517.	481.	461.	453.	451.	454.	457.	458.	457.	45
4458.	4000.	3542.	3097.	2674.	2282.	1925.	1611.	1340.	1114.	932.	792.	690.	621.	579.	559.	553.	558.	569.	582.	593.	599.	593.	58
4464.	4000.	3537.	3088.	2663.	2269.	1915.	1604.	1340.	1124.	953.	826.	739.	684.	657.	650.	657.	673.	693.	713.	730.	738.	730.	71
4469.	4000.	3534.	3082.	2657.	2265.	1915.	1610.	1354.	1148.	990.	876.	802.	761.	747.	752.	769.	792.	817.	841.	859.	867.	859.	84
4475.	4000.	3531.	3080.	2656.	2268.	1923.	1626.	1379.	1184.	1037.	936.	876.	847.	844.	857.	880.	907.	934.	957.	973.	980.	973.	95
4480.	4000.	3529.	3079.	2658.	2276.	1937.	1648.	1411.	1226.	1092.	1003.	954.	936.	940.	959.	984.	1010.	1034.	1053.	1065.	1071.	1065.	105
4486.	4000.	3528.	3079.	2663.	2286.	1955.	1674.	1446.	1271.	1146.	1068.	1029.	1019.	1028.	1048.	1070.	1092.	1109.	1119.	1125.	1128.	1125.	111
4492.	4000.	3527.	3080.	2668.	2297.	1973.	1699.	1478.	1311.	1195.	1125.	1093.	1088.	1098.	1114.	1127.	1140.	1143.	1143.	1143.	1143.	1143.	114
4498.	4000.	3525.	3081.	2673.	2307.	1988.	1720.	1505.	1343.	1232.	1168.	1140.	1135.	1140.	1143.	1143.	1143.	1110.	1110.	1110.	1110.	1110.	111
4504.	4000.	3524.	3081.	2676.	2314.	2000.	1735.	1522.	1363.	1254.	1191.	1163.	1154.	1143.	1110.	1110.	1110.	1110.	0.	0.	0.	0.	
4510.	4000.	3522.	3079.	2677.	2318.	2006.	1743.	1530.	1368.	1257.	1192.	1163.	1143.	1110.	0.	0.	0.	0.	0.	0.	0.	0.	
4516.	4000.	3519.	3077.	2677.	2320.	2009.	1746.	1530.	1363.	1245.	1173.	1143.	1110.	0.	0.	0.	0.	0.	0.	0.	0.	0.	
4524.	4000.	3516.	3074.	2675.	2320.	2010.	1745.	1526.	1354.	1227.	1143.	1110.	0.	0.	0.	0.	0.	0.	0.	0.	0.	0.	
4530.	4000.	3514.	3072.	2674.	2320.	2010.	1745.	1524.	1350.	1223.	1143.	1110.	1124.	0.	0.	0.	0.	0.	0.	0.	0.	0.	
4524.	4000.	3516.	3074.	2675.	2320.	2010.	1745.	1526.	1354.	1227.	1143.	1110.	0.	0.	0.	0.	0.	0.	0.	0.	0.	0.	
4516.	4000.	3519.	3077.	2677.	2320.	2009.	1746.	1530.	1363.	1245.	1173.	1143.	0.	0.	0.	0.	0.	0.	0.	0.	0.	0.	

Figure 16. Stress Function Values for Elliptically Notched Plate

07	-1.76	-0.9
33	-5.65	2.2
56	-5.65	33.6
69	21.82	10.3
23	30.20	31.7
87	27.67	18.3

1.00	1.0
1.05	0.9
0.90	0.9
0.75	0.8
0.50	0.7
0.30	0.7
0.15	0.6
0.05	0.6
0.0	0.6
0.05	0.7
0.15	0.7
0.30	0.9
0.45	1.0
0.70	1.1
0.95	1.3
1.15	1.5
1.40	1.6
1.60	1.7
1.75	1.9
2.00	2.1
2.20	2.2

1.00	1.00	1.00	1.00	1.00	1.00	1.00	1.00	1.00	1.00	1.00	1.00	1.00	1.00	1.00	1.00	1.00	1.00
1.05	1.00	1.10	1.05	1.10	1.05	1.10	1.10	1.00	1.05	1.00	0.95	0.95	0.95	0.90	1.00	0.95	1.00
1.05	1.10	1.15	1.25	1.20	1.20	1.20	1.20	1.10	1.10	1.00	0.90	0.90	0.85	0.75	0.75	1.00	1.10
1.10	1.25	1.30	1.35	1.35	1.45	1.30	1.30	1.25	1.10	1.05	0.90	0.80	0.65	0.65	0.60	0.70	1.50
1.20	1.30	1.45	1.60	1.50	1.60	1.50	1.40	1.40	1.15	1.05	0.85	0.75	0.60	0.55	0.50	0.65	0.80
1.30	1.45	1.60	1.70	1.80	1.70	1.70	1.60	1.40	1.25	1.05	0.85	0.70	0.55	0.35	0.35	0.40	0.60
1.30	1.65	1.70	1.95	1.90	1.90	1.85	1.70	1.55	1.30	1.05	0.85	0.60	0.45	0.30	0.20	0.10	0.30
1.45	1.65	2.00	2.00	2.15	2.00	2.00	1.85	1.55	1.35	1.10	0.80	0.60	0.30	0.25	0.0	-0.10	-0.10
1.55	1.75	2.15	2.15	2.25	2.20	2.10	1.90	1.65	1.35	1.10	0.70	0.55	0.30	0.10	-0.10	-0.25	-0.60
1.55	2.00	2.15	2.35	2.40	2.25	2.20	2.00	1.60	1.40	1.00	0.70	0.45	0.20	0.0	-0.15	-0.45	-0.80
1.65	2.10	2.25	2.45	2.50	2.40	2.20	2.00	1.65	1.35	0.95	0.60	0.30	0.10	-0.05	-0.30	-0.50	-0.80
1.80	2.15	2.40	2.50	2.60	2.40	2.30	2.05	1.55	1.30	0.80	0.50	0.20	0.0	-0.20	-0.35	-0.45	-0.70
1.95	2.15	2.50	2.60	2.60	2.55	2.25	2.00	1.55	1.10	0.75	0.30	0.05	-0.10	-0.25	-0.35	-0.30	-0.60
1.95	2.30	2.50	2.65	2.65	2.50	2.35	1.95	1.45	0.95	0.55	0.10	0.0	-0.25	-0.35	-0.20	-0.15	-0.30
2.05	2.35	2.50	2.65	2.70	2.55	2.30	1.90	1.35	0.75	0.30	-0.15	0.0	-0.50	-0.15	0.0	0.0	0.0
2.10	2.35	2.55	2.65	2.65	2.55	2.35	1.80	1.15	0.50	-0.10	-0.15	0.0	-1.65	0.0	0.0	0.0	0.0
2.15	2.40	2.45	2.60	2.70	2.50	2.30	1.75	0.95	-0.10	-1.10	0.0	0.0	0.0	0.0	0.0	0.0	0.0
2.15	2.35	2.45	2.50	2.55	2.55	2.30	1.80	0.45	-0.65	0.0	0.0	0.0	0.0	0.0	0.0	0.0	0.0
2.15	2.30	2.40	2.35	2.45	2.45	2.30	2.10	0.0	0.0	0.0	0.0	0.0	0.0	0.0	0.0	0.0	0.0
2.20	2.25	2.25	2.30	2.35	2.25	2.15	2.55	0.0	0.0	0.0	0.0	0.0	0.0	0.0	0.0	0.0	0.0
2.20	2.20	2.25	2.20	2.35	2.35	2.35	2.35	0.0	0.0	0.0	0.0	0.0	0.0	0.0	0.0	0.0	0.0

Figure 17. σ_x - Elliptical Cutout

0	0	-0.2
0	0	-0.2
0	0	0.0
0	0	-0.1
0	0	0.0
0	0	0.0
0	0	0.0
0	0	0.0
0	0	0.
0	0	0.
0	0	0.
0	0	0.
0	0	0.
0	0	0.
0	0	-0.
0	0	0.
0	0	-0.
0	0	-0.
0	0	0.
0	0	0.
0	0	0.

-0.85	-1.10	-1.35	-1.50	-1.60	-1.60	-1.55	-1.40	-1.15	-0.90	-0.60	-0.30	-0.05	0.15	0.30	0.35	0.40	0.40
-0.50	-0.70	-0.80	-0.95	-0.95	-0.95	-0.85	-0.75	-0.65	-0.45	-0.25	-0.05	0.15	0.35	0.50	0.60	0.45	0.40
-0.30	-0.40	-0.45	-0.40	-0.45	-0.45	-0.35	-0.25	-0.15	0.0	0.10	0.25	0.45	0.60	0.65	0.75	0.95	0.80
-0.10	-0.05	-0.10	-0.15	-0.05	0.05	0.05	0.15	0.25	0.35	0.50	0.60	0.65	0.75	1.00	1.25	1.55	2.10
0.10	0.10	0.20	0.30	0.25	0.35	0.40	0.45	0.60	0.60	0.65	0.70	0.80	0.90	1.00	1.00	0.95	0.70
0.20	0.25	0.35	0.40	0.60	0.60	0.70	0.75	0.70	0.80	0.85	0.90	0.95	0.95	0.90	1.00	1.10	1.15
0.25	0.45	0.45	0.65	0.65	0.80	0.85	0.90	1.00	0.95	0.90	0.90	0.85	0.90	0.90	0.90	0.85	0.90
0.30	0.40	0.60	0.65	0.80	0.80	0.90	0.95	0.90	0.95	0.95	0.90	0.80	0.65	0.65	0.55	0.55	0.60
0.35	0.40	0.60	0.65	0.75	0.90	0.90	0.90	0.95	0.85	0.80	0.65	0.60	0.50	0.30	0.15	0.05	-0.10
0.25	0.45	0.50	0.65	0.70	0.70	0.80	0.80	0.70	0.70	0.60	0.55	0.40	0.20	0.0	-0.15	-0.40	-0.50
0.25	0.35	0.40	0.50	0.55	0.60	0.50	0.50	0.55	0.45	0.35	0.15	-0.05	-0.20	-0.35	-0.60	-0.75	-0.80
0.15	0.25	0.30	0.30	0.35	0.30	0.40	0.35	0.20	0.15	-0.05	-0.15	-0.35	-0.60	-0.85	-1.00	-1.10	-1.10
0.15	0.10	0.20	0.20	0.15	0.15	-0.05	-0.10	-0.15	-0.30	-0.40	-0.65	-0.90	-1.05	-1.25	-1.50	-1.60	-1.70
0.0	0.05	0.0	-0.05	-0.15	-0.25	-0.25	-0.40	-0.55	-0.70	-0.90	-1.15	-1.45	-1.70	-2.05	-2.10	-2.10	-2.10
0.0	-0.05	-0.15	-0.20	-0.25	-0.40	-0.60	-0.70	-0.85	-1.10	-1.40	-1.85	-2.05	-2.25	-3.35	-2.85	-2.55	-2.40
-0.10	-0.15	-0.15	-0.30	-0.50	-0.60	-0.75	-1.00	-1.20	-1.40	-1.95	-3.10	-2.45	-1.80	0.0	0.0	0.0	0.0
-0.10	-0.15	-0.30	-0.35	-0.45	-0.75	-0.95	-1.10	-1.15	-1.50	-1.80	0.0	0.0	0.0	0.0	0.0	0.0	0.0
-0.05	-0.10	-0.15	-0.25	-0.40	-0.50	-0.75	-1.00	-1.00	-1.10	0.0	0.0	0.0	0.0	0.0	0.0	0.0	0.0
-0.10	-0.10	-0.10	-0.20	-0.20	-0.20	-0.30	-0.55	0.0	0.0	0.0	0.0	0.0	0.0	0.0	0.0	0.0	0.0
0.05	0.0	-0.05	0.05	0.10	0.25	0.70	1.50	0.0	0.0	0.0	0.0	0.0	0.0	0.0	0.0	0.0	0.0
0.10	0.0	0.0	0.0	0.20	0.40	0.40	0.0	0.0	0.0	0.0	0.0	0.0	0.0	0.0	0.0	0.0	0.0

Figure 18. σ_y - Elliptical Cutout

0	0	-0.1
0	0	-0.3
0	0	-0.4
0	0	-0.5
0	0	-0.5
0	0	-0.5
0	0	-0.4
0	0	-0.3
0	0	-0.2
0	0	-0.1
0	0	-0.1
0	0	-0.0
0	0	-0.0
0	0	0.0
0	0	0.0
0	0	0.0
0	0	-0.0
0	0	-0.0
0	0	-0.0
0	0	-0.0
0	0	0.0

0.14	-0.13	-0.10	-0.06	-0.02	0.01	0.05	0.10	0.13	0.14	0.15	0.14	0.11	0.09	0.05	0.02	0.01	0.0
0.36	-0.32	-0.26	-0.16	-0.05	0.05	0.15	0.25	0.32	0.38	0.40	0.38	0.32	0.26	0.16	0.04	-0.02	0.0
0.51	-0.44	-0.32	-0.20	-0.06	0.10	0.25	0.35	0.46	0.54	0.56	0.56	0.51	0.40	0.26	0.10	-0.06	0.0
0.56	-0.47	-0.35	-0.19	-0.02	0.15	0.32	0.45	0.57	0.66	0.69	0.69	0.64	0.54	0.42	0.31	0.16	0.0
0.55	-0.45	-0.32	-0.16	0.04	0.21	0.38	0.55	0.66	0.74	0.77	0.76	0.72	0.67	0.57	0.44	0.30	0.0
0.50	-0.39	-0.24	-0.09	0.10	0.27	0.44	0.60	0.71	0.79	0.82	0.82	0.79	0.71	0.61	0.47	0.26	0.0
0.39	-0.30	-0.15	0.02	0.19	0.35	0.50	0.64	0.74	0.80	0.84	0.84	0.80	0.71	0.63	0.51	0.30	0.0
0.26	-0.17	-0.04	0.13	0.26	0.42	0.56	0.67	0.75	0.79	0.81	0.79	0.74	0.69	0.60	0.47	0.31	0.0
0.15	-0.04	0.09	0.21	0.36	0.49	0.60	0.69	0.74	0.76	0.75	0.70	0.64	0.57	0.49	0.39	0.26	0.0
0.02	0.09	0.20	0.30	0.44	0.55	0.63	0.67	0.70	0.70	0.66	0.60	0.51	0.40	0.31	0.22	0.11	0.0
0.09	0.19	0.29	0.39	0.47	0.56	0.63	0.66	0.66	0.63	0.55	0.45	0.34	0.22	0.13	0.02	-0.02	0.0
0.17	0.26	0.34	0.44	0.50	0.56	0.61	0.63	0.60	0.51	0.40	0.27	0.14	0.02	-0.07	-0.14	-0.10	0.0
0.24	0.31	0.38	0.44	0.49	0.52	0.56	0.55	0.50	0.39	0.24	0.07	-0.07	-0.19	-0.29	-0.29	-0.17	0.0
0.25	0.32	0.38	0.39	0.42	0.45	0.46	0.45	0.38	0.24	0.04	-0.19	-0.31	-0.42	-0.50	-0.39	-0.22	0.0
0.24	0.29	0.31	0.32	0.32	0.34	0.35	0.31	0.20	0.01	-0.26	-0.49	-0.55	-0.90	-0.75	-0.20	-0.11	0.0
0.20	0.24	0.24	0.21	0.20	0.19	0.17	0.14	0.0	-0.31	-0.88	-0.77	-0.32	-0.20	0.0	0.0	0.0	0.0
0.16	0.17	0.15	0.09	0.02	0.0	-0.01	-0.02	-0.20	-0.66	0.0	0.0	0.0	0.0	0.0	0.0	0.0	0.0
0.13	0.10	0.06	-0.01	-0.14	-0.21	-0.22	-0.14	-0.32	0.0	0.0	0.0	0.0	0.0	0.0	0.0	0.0	0.0
0.09	0.07	0.0	-0.10	-0.20	-0.32	-0.44	-0.29	0.0	0.0	0.0	0.0	0.0	0.0	0.0	0.0	0.0	0.0
0.06	0.05	-0.01	-0.09	-0.15	-0.20	-0.21	-0.14	0.0	0.0	0.0	0.0	0.0	0.0	0.0	0.0	0.0	0.0
0.0	0.0	0.0	0.0	0.0	0.0	0.0	0.0	0.0	0.0	0.0	0.0	0.0	0.0	0.0	0.0	0.0	0.0

Figure 19. τ_{xy} - Elliptical Cutout

1.00	1.0
1.05	1.0
0.90	1.1
0.75	1.0
0.50	1.0
0.30	0.9
0.15	0.8
0.05	0.7
0.0	0.7
0.05	0.7
0.15	0.7
0.30	0.9
0.45	1.0
0.70	1.1
0.95	1.3
1.15	1.5
1.40	1.6
1.60	1.7
1.75	1.9
2.00	2.1
2.20	2.2

1.01	1.01	1.00	1.00	1.00	1.00	1.00	1.00	1.01	1.01	1.01	1.01	1.01	1.01	1.00	1.00	1.00	1.00
1.13	1.06	1.13	1.06	1.10	1.05	1.11	1.13	1.06	1.14	1.12	1.08	1.06	1.05	0.96	1.00	0.95	1.00
1.22	1.22	1.21	1.27	1.20	1.21	1.24	1.28	1.25	1.32	1.27	1.22	1.23	1.14	0.96	0.85	1.04	1.10
1.32	1.40	1.38	1.37	1.35	1.47	1.38	1.46	1.51	1.48	1.52	1.46	1.37	1.24	1.28	1.37	1.58	2.10
1.43	1.45	1.53	1.62	1.50	1.63	1.62	1.65	1.77	1.66	1.65	1.54	1.50	1.44	1.39	1.26	1.14	0.80
1.49	1.57	1.64	1.71	1.81	1.76	1.87	1.91	1.84	1.85	1.78	1.70	1.62	1.49	1.29	1.25	1.19	1.15
1.43	1.72	1.72	1.95	1.93	2.00	2.06	2.05	2.06	1.94	1.82	1.72	1.53	1.42	1.30	1.17	0.96	0.90
1.51	1.67	2.00	2.01	2.20	2.13	2.23	2.21	2.04	1.96	1.84	1.64	1.45	1.19	1.08	0.82	0.67	0.60
1.57	1.75	2.16	2.18	2.33	2.36	2.35	2.25	2.12	1.90	1.71	1.38	1.22	0.98	0.70	0.43	0.20	-0.10
1.55	2.01	2.17	2.40	2.51	2.43	2.44	2.30	1.98	1.83	1.49	1.23	0.94	0.60	0.31	0.07	-0.31	-0.50
1.66	2.12	2.29	2.53	2.61	2.56	2.41	2.25	1.96	1.67	1.28	0.88	0.51	0.22	0.0	-0.30	-0.50	-0.80
1.82	2.18	2.45	2.58	2.71	2.54	2.48	2.26	1.78	1.49	0.96	0.60	0.23	0.0	-0.19	-0.32	-0.43	-0.70
1.98	2.20	2.56	2.68	2.69	2.66	2.38	2.14	1.69	1.20	0.80	0.31	0.06	-0.06	-0.17	-0.28	-0.28	-0.60
1.98	2.34	2.56	2.71	2.71	2.57	2.43	2.03	1.52	0.98	0.55	0.13	0.06	-0.14	-0.21	-0.12	-0.13	-0.30
2.08	2.38	2.54	2.69	2.73	2.59	2.34	1.94	1.37	0.75	0.34	-0.02	0.14	-0.12	0.02	0.01	0.0	0.0
2.12	2.37	2.57	2.66	2.66	2.56	2.36	1.81	0.0	0.0	0.0	0.0	0.0	0.0	0.0	0.0	0.0	0.0
2.16	2.41	2.46	2.60	2.70	2.50	2.30	1.75	0.97	0.16	-1.10	0.0	0.0	0.0	0.0	0.0	0.0	0.0
2.16	2.35	2.45	2.50	2.56	2.56	2.32	1.81	0.52	-0.65	0.0	0.0	0.0	0.0	0.0	0.0	0.0	0.0
2.15	2.30	2.40	2.35	2.47	2.49	2.37	2.13	0.0	0.0	0.0	0.0	0.0	0.0	0.0	0.0	0.0	0.0
2.20	2.25	2.25	2.30	2.36	2.27	2.18	2.57	0.0	0.0	0.0	0.0	0.0	0.0	0.0	0.0	0.0	0.0
2.20	2.20	2.25	2.20	2.35	2.35	2.35	2.35	0.0	0.0	0.0	0.0	0.0	0.0	0.0	0.0	0.0	0.0

Figure 20. σ_{p_1} - Elliptical Cutout

.07	-1.76	-0.9
.33	-5.65	2.2
.56	-5.65	33.6
.69	21.82	10.3
.23	30.20	31.7
.87	27.67	18.3

0	0	-0.
0	0	-0.
0	0	-0.
0	0	-0.
0	0	-0.
0	0	-0.
0	0	-0.
0	0	-0.
0	0	-0.
0	0	0.
0	0	-0.
0	0	0.
0	0	0.
0	0	0.
0	0	-0.
0	0	0.
0	0	-0.
0	0	-0.
0	0	0
0	0	0
0	0	0

-0.86	-1.11	-1.35	-1.50	-1.60	-1.60	-1.55	-1.40	-1.16	-0.91	-0.61	-0.31	-0.06	0.14	0.30	0.35	0.40	0.40
-0.58	-0.76	-0.83	-0.96	-0.95	-0.95	-0.86	-0.78	-0.71	-0.54	-0.37	-0.18	0.04	0.25	0.44	0.60	0.45	0.40
-0.47	-0.52	-0.51	-0.42	-0.45	-0.46	-0.39	-0.33	-0.30	-0.22	-0.17	-0.07	0.12	0.31	0.44	0.65	0.91	0.80
-0.32	-0.20	-0.18	-0.17	-0.05	0.03	-0.03	-0.01	-0.01	-0.03	0.03	0.04	0.08	0.16	0.37	0.48	0.67	1.50
-0.13	-0.05	0.12	0.28	0.25	0.32	0.28	0.20	0.23	0.09	0.05	0.01	0.05	0.06	0.16	0.24	0.46	0.70
0.01	0.13	0.31	0.39	0.59	0.54	0.53	0.44	0.26	0.20	0.12	0.05	0.03	0.01	-0.04	0.10	0.31	0.60
0.12	0.38	0.43	0.65	0.62	0.70	0.64	0.55	0.49	0.31	0.13	0.03	-0.08	-0.07	-0.10	-0.07	-0.01	0.30
0.24	0.38	0.60	0.64	0.75	0.67	0.67	0.59	0.41	0.34	0.21	0.06	-0.05	-0.24	-0.18	-0.27	-0.22	-0.10
0.33	0.40	0.59	0.62	0.67	0.74	0.65	0.55	0.48	0.30	0.19	-0.03	-0.07	-0.18	-0.30	-0.38	-0.40	-0.60
0.25	0.44	0.48	0.60	0.59	0.52	0.56	0.50	0.32	0.27	0.11	0.02	-0.09	-0.20	-0.31	-0.37	-0.54	-0.80
0.24	0.33	0.36	0.42	0.44	0.44	0.29	0.25	0.24	0.13	0.02	-0.13	-0.26	-0.32	-0.40	-0.60	-0.75	-0.80
0.13	0.22	0.25	0.22	0.24	0.16	0.22	0.14	-0.03	-0.04	-0.21	-0.25	-0.38	-0.60	-0.86	-1.03	-1.12	-1.10
0.12	0.05	0.14	0.12	0.06	0.04	-0.18	-0.24	-0.29	-0.40	-0.45	-0.66	-0.91	-1.09	-1.33	-1.57	-1.62	-1.70
-0.03	0.01	-0.06	-0.11	-0.21	-0.32	-0.33	-0.48	-0.62	-0.73	-0.90	-1.18	-1.51	-1.81	-2.19	-2.18	-2.12	-2.10
-0.03	-0.08	-0.19	-0.24	-0.28	-0.44	-0.64	-0.74	-0.87	-1.10	-1.44	-1.98	-2.19	-2.63	-3.52	-2.86	-2.55	-2.40
-0.12	-0.17	-0.17	-0.31	-0.51	-0.61	-0.76	-1.01	0.0	0.0	0.0	0.0	0.0	0.0	0.0	0.0	0.0	0.0
-0.11	-0.16	-0.31	-0.35	-0.45	-0.75	-0.95	-1.10	-1.17	-1.76	-1.80	0.0	0.0	0.0	0.0	0.0	0.0	0.0
-0.06	-0.10	-0.15	-0.25	-0.41	-0.51	-0.77	-1.01	-1.07	-1.10	0.0	0.0	0.0	0.0	0.0	0.0	0.0	0.0
-0.10	-0.10	-0.10	-0.20	-0.22	-0.24	-0.37	-0.58	0.0	0.0	0.0	0.0	0.0	0.0	0.0	0.0	0.0	0.0
0.05	0.0	-0.05	0.05	0.09	0.23	0.67	1.48	0.0	0.0	0.0	0.0	0.0	0.0	0.0	0.0	0.0	0.0
0.10	0.0	0.0	0.0	0.20	0.40	0.40	0.0	0.0	0.0	0.0	0.0	0.0	0.0	0.0	0.0	0.0	0.0

Figure 21. σ_{P_2} - Elliptical Cutout

4410.	4000.	3610.	3240.	2890.	2560.	2250.	1960.	1690.	1440.	1210.	1000.	810.	640.	490.	360.	250.	160.	90.	40.	10.	0.	10.	4
4410.	4000.	3610.	3240.	2890.	2560.	2250.	1960.	1690.	1440.	1210.	1000.	810.	640.	490.	360.	250.	160.	90.	40.	10.	0.	10.	4
4416.	4C00.	3605.	3232.	2878.	2546.	2234.	1944.	1675.	1428.	1202.	997.	814.	651.	508.	386.	283.	199.	134.	88.	61.	51.	61.	8
4423.	4000.	3599.	3219.	2860.	2524.	2210.	1920.	1654.	1412.	1193.	997.	824.	674.	544.	434.	343.	270.	215.	175.	152.	144.	152.	17
4429.	4C0C.	3590.	3204.	2839.	2498.	2183.	1894.	1613.	1396.	1186.	1003.	845.	710.	596.	503.	428.	369.	324.	293.	275.	269.	275.	29
4436.	4000.	3583.	3188.	2817.	2473.	2156.	1869.	1611.	1384.	1186.	1017.	875.	758.	664.	590.	532.	488.	457.	435.	422.	418.	422.	43
4442.	4000.	3576.	3174.	2797.	2449.	2132.	1848.	1596.	1378.	1194.	1040.	916.	819.	745.	691.	652.	624.	606.	594.	587.	584.	587.	59
4449.	4000.	3569.	3161.	2779.	2429.	2113.	1832.	1587.	1380.	1209.	1072.	966.	889.	836.	801.	781.	770.	764.	761.	759.	758.	759.	76
4455.	4000.	3563.	3149.	2764.	2413.	2098.	1821.	1585.	1388.	1231.	1110.	1023.	965.	931.	915.	912.	916.	922.	926.	928.	928.	928.	92
4462.	4C00.	3557.	3139.	2752.	24CC.	2087.	1815.	1587.	1401.	1257.	1152.	1082.	1041.	1025.	1026.	1037.	1053.	1068.	1076.	1080.	1081.	1080.	107
4468.	4000.	3552.	3130.	2741.	2390.	2080.	1814.	1593.	1418.	1286.	1194.	1139.	1113.	1111.	1124.	1145.	1168.	1188.	1196.	1198.	1199.	1198.	119
4474.	4000.	3547.	3123.	2733.	2382.	2075.	1814.	1601.	1434.	1313.	1233.	1189.	1174.	1181.	1200.	1224.	1244.	1264.	1264.	1264.	1264.	1264.	126
4481.	4CC0.	3543.	3116.	2726.	2376.	2072.	1816.	1608.	1449.	1336.	1264.	1228.	1220.	1230.	1248.	1264.	1264.	1258.	1258.	1258.	1258.	1258.	125
4487.	4000.	3539.	3110.	2719.	2371.	2069.	1816.	1613.	1459.	1350.	1286.	1255.	1250.	1257.	1264.	1258.	1258.	0.	0.	0.	0.	0.	
4494.	4CC0.	3535.	3104.	2712.	2365.	2065.	1814.	1614.	1463.	1359.	1297.	1268.	1263.	1264.	1258.	0.	0.	0.	0.	0.	0.	0.	
4500.	4C00.	3531.	3097.	2705.	2358.	2059.	1810.	1611.	1461.	1358.	1297.	1270.	1264.	1258.	0.	0.	0.	0.	0.	0.	0.	0.	
4507.	4000.	3527.	3091.	2698.	2351.	2052.	1803.	1604.	1454.	1351.	1290.	1264.	1258.	0.	0.	0.	0.	0.	0.	0.	0.	0.	
4513.	4CC0.	3523.	3085.	2691.	2344.	2045.	1795.	1595.	1444.	1339.	1280.	1264.	1258.	0.	0.	0.	0.	0.	0.	0.	0.	0.	
4520.	4000.	3519.	3080.	2685.	2337.	203[illegible]	1788.	1586.	1433.	1326.	1264.	1258.	0.	0.	0.	0.	0.	0.	0.	0.	0.	0.	
4526.	4000.	3516.	3075.	2680.	2332.	2032.	1782.	1580.	1427.	1321.	1264	1258.	0.	0.	0.	0.	0.	0.	0.	0.	0.	0.	
4533.	4000.	3514.	3072.	2676.	2328.	2029.	1778.	1577.	1424.	1320.	1264	1258.	0.	0.	0.	0.	0.	0.	0.	0.	0.	0.	
4533.	4C00.	3513.	3071.	2675.	2327.	2027.	1777.	1575.	1423.	1319.	1264	1258.	1302.	0.	0.	0.	0.	0.	0.	0.	0.	0.	
4533.	4000.	3514.	3072.	2676.	2328.	2029.	1778.	1577.	1424.	1320.	1264.	1258.	0.	0.	0.	0.	0.	0.	0.	0.	0.	0.	
4526.	4000.	3516.	3075.	2680.	2332.	2032.	1782.	1580.	1427.	1321.	1264.	1258.	0.	0.	0.	0.	0.	0.	0.	0.	0.	0.	

Figure 23. Stress Function Values For Circularly Notched Plate

.00	1.00	1.00	1.00	1.00	1.00	1.00	1.00	1.00	1.00	1.00	1.00	1.00	1.00	1.00	1.00	1.00	1.00	1.00
.95	1.10	1.00	1.10	1.05	1.10	1.05	1.05	1.10	1.00	1.00	1.05	0.95	0.95	0.95	0.95	0.95	0.85	1.00
.05	1.15	1.10	1.20	1.20	1.20	1.15	1.15	1.15	1.15	1.00	1.00	0.95	0.90	0.90	0.75	0.85	0.75	0.80
.10	1.20	1.30	1.30	1.30	1.40	1.25	1.35	1.25	1.15	1.05	1.05	0.90	0.80	0.70	0.70	0.65	0.60	0.60
.20	1.35	1.35	1.50	1.45	1.55	1.45	1.45	1.35	1.25	1.15	1.00	0.80	0.70	0.65	0.45	0.45	0.45	0.40
.25	1.45	1.55	1.65	1.60	1.70	1.70	1.50	1.50	1.35	1.15	1.00	0.75	0.55	0.50	0.30	0.25	0.20	0.30
.30	1.60	1.70	1.75	1.80	1.90	1.80	1.70	1.55	1.45	1.20	0.90	0.75	0.45	0.25	0.15	0.05	0.05	0.10
.45	1.70	1.80	1.90	2.05	1.95	2.00	1.80	1.70	1.45	1.20	0.90	0.65	0.35	0.10	-0.10	-0.10	-0.10	0.0
.55	1.75	1.95	2.05	2.20	2.10	2.10	1.95	1.75	1.45	1.25	0.85	0.50	0.25	-0.05	-0.35	-0.20	-0.15	-0.10
.65	1.90	2.05	2.20	2.25	2.30	2.15	2.00	1.85	1.45	1.20	0.75	0.40	0.10	-0.15	-0.60	-0.30	-0.05	-0.10
.70	1.95	2.20	2.30	2.40	2.30	2.30	2.05	1.80	1.45	1.10	0.60	0.25	-0.20	0.0	-1.00	0.0	0.0	0.0
.85	2.00	2.30	2.40	2.40	2.45	2.30	2.05	1.80	1.40	0.90	0.40	-0.10	-0.80	-0.30	0.0	0.0	0.0	0.0
.90	2.15	2.30	2.45	2.5	2.45	2.30	2.15	1.70	1.30	0.60	0.0	-0.65	0.0	0.0	0.0	0.0	0.0	0.0
.95	2.25	2.35	2.45	2.55	2.45	2.35	2.10	1.65	1.20	0.30	-0.35	0.0	0.0	0.0	0.0	0.0	0.0	0.0
.10	2.25	2.40	2.50	2.50	2.45	2.35	2.10	1.70	1.05	0.0	0.0	0.0	0.0	0.0	0.0	0.0	0.0	0.0
.15	2.30	2.40	2.50	2.50	2.45	2.35	2.10	1.75	1.00	0.0	0.0	0.0	0.0	0.0	0.0	0.0	0.0	0.0
.20	2.35	2.40	2.45	2.50	2.45	2.30	2.30	2.15	0.50	0.0	0.0	0.0	0.0	0.0	0.0	0.0	0.0	0.0
.20	2.35	2.45	2.45	2.40	2.45	2.30	2.25	2.80	0.0	0.0	0.0	0.0	0.0	0.0	0.0	0.0	0.0	0.0
.30	2.35	2.40	2.50	2.40	2.45	2.35	2.45	2.55	0.0	0.0	0.0	0.0	0.0	0.0	0.0	0.0	0.0	0.0
.30	2.40	2.45	2.40	2.50	2.40	2.45	2.40	2.50	0.0	0.0	0.0	0.0	0.0	0.0	0.0	0.0	0.0	0.0
.30	2.40	2.40	2.50	2.40	2.50	2.40	2.45	2.45	0.0	0.0	0.0	0.0	0.0	0.0	0.0	0.0	0.0	0.0

Figure 24. σ_x - Circular Cutout

.40	-0.60	-0.70	-0.80	-0.80	-0.75	-0.60	-0.40	-0.15	0.20	0.55	0.90	1.30	1.65	1.95	2.20	2.40	2.55	2.55
.25	-0.30	-0.40	-0.40	-0.40	-0.30	-0.20	-0.05	0.15	0.30	0.60	0.90	1.10	1.35	1.60	1.85	1.95	2.00	2.10
.10	-0.15	-0.20	-0.15	-0.10	-0.10	0.0	0.10	0.30	0.55	0.65	0.80	1.05	1.25	1.40	1.40	1.55	1.60	1.60
.05	-0.05	0.05	0.0	0.05	0.15	0.20	0.35	0.40	0.45	0.60	0.80	0.90	0.95	1.00	1.20	1.20	1.20	1.20
.10	0.10	0.05	0.15	0.20	0.25	0.30	0.40	0.45	0.55	0.65	0.65	0.70	0.80	0.85	0.80	0.85	0.90	0.85
.05	0.10	0.20	0.25	0.25	0.30	0.40	0.35	0.45	0.45	0.45	0.50	0.45	0.45	0.50	0.45	0.40	0.35	0.40
.05	0.15	0.20	0.20	0.25	0.35	0.30	0.35	0.30	0.35	0.30	0.20	0.20	0.10	0.0	0.0	-0.10	-0.15	-0.20
.10	0.15	0.15	0.20	0.25	0.20	0.25	0.20	0.20	0.10	0.0	-0.05	-0.15	-0.30	-0.45	-0.60	-0.75	-0.85	-0.85
.05	0.05	0.15	0.20	0.25	0.20	0.20	0.15	0.0	-0.10	-0.20	-0.40	-0.65	-0.85	-1.10	-1.30	-1.50	-1.70	-1.75
.10	0.15	0.10	0.10	0.05	0.10	-0.05	-0.10	-0.15	-0.35	-0.55	-0.80	-1.10	-1.45	-1.95	-2.20	-2.60	-2.60	-2.65
.0	0.05	0.10	0.10	0.10	-0.05	-0.05	-0.20	-0.40	-0.55	-0.75	-1.05	-1.40	-1.95	-2.80	-4.10	-3.70	-3.60	-3.55
.05	0.0	0.05	0.0	-0.10	-0.10	-0.25	-0.40	-0.45	-0.60	-0.80	-1.10	-1.60	-2.30	-1.30	0.0	0.0	0.0	0.0
.0	0.0	-0.05	-0.05	-0.10	-0.20	-0.30	-0.35	-0.55	-0.70	-0.85	-1.00	-1.10	0.0	0.0	0.0	0.0	0.0	0.0
.05	0.0	-0.05	-0.10	-0.10	-0.20	-0.30	-0.45	-0.55	-0.55	-0.60	-0.65	0.0	0.0	0.0	0.0	0.0	0.0	0.0
.05	0.0	0.0	-0.05	-0.15	-0.20	-0.25	-0.30	-0.35	-0.40	-0.35	0.0	0.0	0.0	0.0	0.0	0.0	0.0	0.0
.0	0.0	0.0	0.0	-0.05	-0.10	-0.15	-0.25	-0.15	0.30	0.0	0.0	0.0	0.0	0.0	0.0	0.0	0.0	0.0
.05	0.05	0.0	0.0	0.05	0.0	-0.05	-0.05	-0.30	-0.30	0.0	0.0	0.0	0.0	0.0	0.0	0.0	0.0	0.0
.0	0.05	0.10	0.05	0.05	0.15	0.25	0.40	0.80	0.0	0.0	0.0	0.0	0.0	0.0	0.0	0.0	0.0	0.0
.10	0.05	0.05	0.15	0.10	0.15	0.15	0.20	0.0	0.0	0.0	0.0	0.0	0.0	0.0	0.0	0.0	0.0	0.0
.10	0.15	0.15	0.05	0.15	0.05	0.10	0.0	0.0	0.0	0.0	0.0	0.0	0.0	0.0	0.0	0.0	0.0	0.0
.10	0.10	0.10	0.20	0.10	0.20	0.10	0.10	0.0	0.0	0.0	0.0	0.0	0.0	0.0	0.0	0.0	0.0	0.0

Figure 25. σ_y - Circular Cutout

.09	-0.07	-0.05	-0.02	0.01	0.05	0.09	0.11	0.15	0.17	0.17	0.19	0.19	0.16	0.14	0.11	0.09	0.04	0.0
.24	-0.19	-0.13	-0.05	0.05	0.15	0.24	0.31	0.39	0.46	0.50	0.50	0.49	0.45	0.40	0.31	0.21	0.11	0.0
.30	-0.25	-0.15	-0.02	-0.14	0.22	0.57	0.47	0.59	0.66	0.71	0.72	0.71	0.66	0.56	0.44	0.30	0.16	0.0
.34	-0.25	-0.14	0.0	0.14	0.29	0.45	0.60	0.72	0.80	0.86	0.90	0.86	0.77	0.66	0.52	0.35	0.17	0.0
.35	-0.24	-0.11	0.04	0.42	0.35	0.31	0.69	0.79	0.90	0.97	0.99	0.94	0.84	0.72	0.57	0.38	0.17	0.0
.30	-0.21	-0.06	0.09	0.24	0.41	0.59	0.74	0.85	0.95	1.01	1.00	0.96	0.89	0.72	0.55	0.38	0.17	0.0
.25	-0.14	-0.01	0.11	0.29	0.46	0.60	0.75	0.88	0.95	0.99	0.97	0.92	0.85	0.70	0.50	0.31	0.15	0.0
.19	-0.09	0.01	0.15	0.32	0.47	0.60	0.74	0.85	0.90	0.91	0.91	0.84	0.72	0.60	0.40	0.21	0.10	0.0
.15	-0.05	0.06	0.20	0.32	0.46	0.59	0.67	0.76	0.80	0.80	0.76	0.66	0.54	0.41	0.22	0.05	0.01	0.0
.11	-0.02	0.09	0.21	0.32	0.42	0.52	0.60	0.64	0.65	0.61	0.51	0.39	0.21	0.11	-0.04	-0.15	-0.06	0.0
.07	0.0	0.09	0.20	0.29	0.36	0.44	0.49	0.49	0.46	0.38	0.21	0.0	-0.35	-0.61	-0.42	-0.13	-0.04	0.0
.07	0.02	0.10	0.16	0.22	0.29	0.31	0.35	0.36	0.29	0.13	-0.15	-0.52	-0.63	0.0	0.0	0.0	0.0	0.0
.07	0.01	0.09	0.11	0.16	0.20	0.21	0.24	0.21	0.13	-0.07	-0.41	0.0	0.0	0.0	0.0	0.0	0.0	0.0
.07	0.0	0.05	0.09	0.10	0.10	0.13	0.11	0.09	0.04	-0.17	0.0	0.0	0.0	0.0	0.0	0.0	0.0	0.0
.07	-0.01	0.01	0.04	0.04	0.02	0.02	0.02	0.05	0.02	0.0	0.0	0.0	0.0	0.0	0.0	0.0	0.0	0.0
.07	-0.02	0.0	-0.01	-0.02	-0.02	-0.04	0.0	0.16	0.14	0.0	0.0	0.0	0.0	0.0	0.0	0.0	0.0	0.0
.06	-0.04	-0.01	-0.01	-0.05	-0.07	-0.09	-0.06	0.24	0.0	0.0	0.0	0.0	0.0	0.0	0.0	0.0	0.0	0.0
.05	-0.02	-0.02	-0.01	-0.02	-0.05	-0.04	0.01	0.15	0.0	0.0	0.0	0.0	0.0	0.0	0.0	0.0	0.0	0.0
.05	-0.01	0.0	-0.01	0.0	0.01	0.04	0.11	0.07	0.0	0.0	0.0	0.0	0.0	0.0	0.0	0.0	0.0	0.0
.02	-0.01	0.0	0.0	0.0	0.01	0.04	0.05	0.02	0.0	0.0	0.0	0.0	0.0	0.0	0.0	0.0	0.0	0.0
.0	0.0	0.0	0.0	0.0	0.0	0.0	0.0	0.0	0.0	0.0	0.0	0.0	0.0	0.0	0.0	0.0	0.0	0.0

Figure 26. τ_{xy} - Circular Cutout

01	1.00	1.00	1.00	1.00	1.00	1.01	1.01	1.02	1.03	1.06	1.15	1.39	1.69	1.97	2.21	2.41	2.55	2.55
00	1.13	1.01	1.10	1.05	1.12	1.09	1.13	1.24	1.23	1.34	1.48	1.52	1.64	1.79	1.95	1.99	2.01	2.10
12	1.20	1.12	1.20	1.21	1.24	1.38	1.33	1.45	1.57	1.56	1.63	1.71	1.76	1.76	1.62	1.66	1.63	1.60
19	1.25	1.32	1.30	1.32	1.46	1.42	1.63	1.66	1.67	1.71	1.83	1.76	1.65	1.53	1.53	1.37	1.24	1.20
30	1.39	1.36	1.50	1.58	1.64	1.53	1.79	1.81	1.87	1.90	1.83	1.69	1.59	1.48	1.22	1.08	0.96	0.85
32	1.48	1.55	1.66	1.64	1.81	1.93	1.86	1.97	1.95	1.87	1.78	1.57	1.39	1.22	0.93	0.71	0.46	0.40
35	1.61	1.70	1.76	1.85	2.03	2.01	2.03	2.00	2.00	1.84	1.58	1.44	1.14	0.84	0.58	0.29	0.13	0.10
48	1.71	1.80	1.91	2.11	2.07	2.19	2.09	2.08	1.90	1.69	1.45	1.18	0.81	0.49	0.12	-0.04	-0.09	0.0
56	1.75	1.95	2.07	2.25	2.21	2.27	2.17	2.03	1.79	1.60	1.21	0.80	0.47	0.09	-0.30	-0.20	-0.15	-0.10
66	1.90	2.05	2.22	2.30	2.38	2.27	2.16	2.04	1.66	1.39	0.90	0.50	0.13	-0.14	-0.60	-0.29	-0.05	-0.10
70	1.95	2.20	2.32	2.44	2.35	2.38	2.15	1.90	1.55	1.18	0.63	0.25	-0.13	0.13	-0.94	0.0	0.0	0.0
85	2.00	2.30	2.41	2.42	2.48	2.34	2.10	1.86	0.0	0.91	0.41	0.06	-0.57	0.0	0.0	0.0	0.0	0.0
90	2.15	2.30	2.45	2.51	2.47	2.32	2.17	1.72	1.31	0.60	0.15	0.0	0.0	0.0	0.0	0.0	0.0	0.0
95	2.25	2.35	2.45	2.55	2.45	2.36	2.10	1.65	1.20	0.33	0.0	0.0	0.0	0.0	0.0	0.0	0.0	0.0
10	2.25	2.40	2.50	2.50	2.45	2.35	2.10	1.70	1.05	0.0	0.0	0.0	0.0	0.0	0.0	0.0	0.0	0.0
15	2.30	2.40	2.50	2.50	2.45	2.35	2.10	1.76	1.03	0.0	0.0	0.0	0.0	0.0	0.0	0.0	0.0	0.0
20	2.35	2.40	2.45	2.50	2.45	2.30	2.30	2.17	0.0	0.0	0.0	0.0	0.0	0.0	0.0	0.0	0.0	0.0
20	2.35	2.45	2.45	2.40	2.45	2.30	2.25	2.81	0.0	0.0	0.0	0.0	0.0	0.0	0.0	0.0	0.0	0.0
30	2.35	2.40	2.50	2.40	2.45	2.35	2.46	2.55	0.0	0.0	0.0	0.0	0.0	0.0	0.0	0.0	0.0	0.0
30	2.40	2.45	2.40	2.50	2.40	2.45	2.40	2.50	0.0	0.0	0.0	0.0	0.0	0.0	0.0	0.0	0.0	0.0
30	2.40	2.40	2.50	2.40	2.50	2.40	2.45	2.45	0.0	0.0	0.0	0.0	0.0	0.0	0.0	0.0	0.0	0.0

Figure 27. σ_{p_1} - Circular Cutout

.41	-0.60	-0.70	-0.80	-0.8(	-0.75	-0.61	-0.41	-0.17	0.17	0.49	0.75	0.91	0.96	0.98	0.99	0.99	1.00	1.00
.30	-0.33	-0.41	-0.40	-0.40	-0.32	-0.24	-0.13	0.01	0.07	0.26	0.47	0.53	0.66	0.76	0.85	0.91	0.84	1.00
.17	-0.20	-0.22	-0.15	-0.11	-0.14	-0.23	-0.08	0.0	0.13	0.09	0.17	0.29	0.39	0.54	0.53	0.74	0.72	0.80
.14	-0.10	0.03	0.0	0.03	0.09	0.03	0.07	-0.01	-0.07	-0.06	0.02	0.04	0.10	0.17	0.37	0.48	0.56	0.60
.0	0.06	0.04	0.15	0.07	0.16	0.22	0.06	-0.01	-0.07	-0.10	-0.18	-0.19	-0.09	0.02	0.03	0.22	0.39	0.40
.02	0.07	0.20	0.24	0.21	0.19	0.17	-0.01	-0.02	-0.15	-0.27	-0.28	-0.37	-0.39	-0.22	-0.18	-0.06	0.09	0.30
.0	0.14	0.20	0.19	0.20	0.22	0.09	0.02	-0.15	-0.20	-0.34	-0.48	-0.49	-0.59	-0.59	-0.43	-0.34	-0.23	-0.20
.07	0.14	0.15	0.19	0.19	0.08	0.06	-0.09	-0.18	-0.35	-0.49	-0.60	-0.68	-0.76	-0.84	-0.82	-0.81	-0.86	-0.85
.04	0.05	0.15	0.18	0.20	0.09	0.03	-0.07	-0.28	-0.44	-0.55	-0.76	-0.95	-1.07	-1.24	-1.35	-1.50	-1.70	-1.75
.09	0.15	0.10	0.08	0.0	0.02	-0.17	-0.26	-0.34	-0.56	-0.74	-0.95	-1.20	-1.48	-1.96	-2.20	-2.61	-2.60	-2.65
.0	0.05	0.10	0.08	0.06	-0.10	-0.13	-0.30	-0.50	-0.65	-0.83	-1.08	-1.40	-2.02	-2.93	-4.16	-3.70	-3.60	-3.55
.05	0.0	0.05	-0.01	-0.12	-0.13	-0.29	-0.45	-0.51	0.0	-0.81	-1.11	-1.76	-2.53	0.0	0.0	0.0	0.0	0.0
.0	0.0	-0.05	-0.05	-0.11	-0.22	-0.32	-0.37	-0.57	-0.71	-0.85	-1.15	0.0	0.0	0.0	0.0	0.0	0.0	0.0
.05	0.0	-0.05	-0.10	-0.10	-0.20	-0.31	-0.45	-0.55	-0.55	-0.63	0.0	0.0	0.0	0.0	0.0	0.0	0.0	0.0
.05	0.0	0.0	-0.05	-0.15	-0.20	-0.25	-0.30	-0.35	-0.40	0.0	0.0	0.0	0.0	0.0	0.0	0.0	0.0	0.0
.0	0.0	0.0	0.0	-0.05	-0.10	-0.15	-0.25	-0.16	0.27	0.0	0.0	0.0	0.0	0.0	0.0	0.0	0.0	0.0
.05	0.05	0.0	0.0	0.05	0.0	-0.05	-0.05	-0.32	0.0	0.0	0.0	0.0	0.0	0.0	0.0	0.0	0.0	0.0
.0	0.05	0.10	0.05	0.05	0.15	0.25	0.40	0.79	0.0	0.0	0.0	0.0	0.0	0.0	0.0	0.0	0.0	0.0
.10	0.05	0.05	0.15	0.10	0.15	0.15	0.19	0.0	0.0	0.0	0.0	0.0	0.0	0.0	0.0	0.0	0.0	0.0
.10	0.15	0.15	0.05	0.15	0.05	0.10	0.0	0.0	0.0	0.0	0.0	0.0	0.0	0.0	0.0	0.0	0.0	0.0
.10	0.10	0.10	0.20	0.10	0.20	0.10	0.10	0.0	0.0	0.0	0.0	0.0	0.0	0.0	0.0	0.0	0.0	0.0

Figure 28. σ_{p_2} - Circular Cutout

0.0	4.55	3.66	2.50	1.68	0.64	-0.32	-1.64	-3.21	-4.47	-7.31	-11.51	-18.54	-37.63	25.86	13.11	8.21	5.19	3.66	1.4
0.0	12.17	10.90	7.59	5.26	1.91	-1.97	-6.05	-10.50	-14.70	-19.69	-26.37	-34.10	-40.73	40.65	33.02	25.45	17.28	11.39	5.4
0.0	15.66	13.78	10.52	6.50	0.85	6.08	-9.35	-22.37	-20.92	-27.12	-32.78	-38.08	-41.05	42.99	37.57	32.97	26.77	20.30	10.3
0.0	17.67	15.30	10.90	6.31	0.0	-6.31	-12.45	-20.30	-25.10	-29.72	-33.19	-37.67	-41.05	-29.91	42.22	38.60	32.16	25.92	14.7
0.0	17.95	16.24	10.50	4.80	-1.70	-16.95	-14.15	-14.17	-26.37	-30.17	-34.37	-37.77	-39.99	-43.48	43.30	41.05	36.47	31.12	18.5
0.0	15.86	13.28	8.64	2.54	-3.66	-9.79	-15.18	-21.11	-26.08	-29.15	-32.33	-35.44	-37.98	-40.56	-43.39	-27.61	41.12	39.42	33.1
0.0	14.70	10.90	5.46	0.38	-4.04	-10.26	-15.35	-19.33	-24.01	-27.31	-29.97	-32.78	-35.08	-36.68	-39.18	-39.94	-40.73	-38.20	-28.1
0.0	12.58	7.86	3.31	-0.35	-5.00	-9.79	-14.12	-17.22	-21.38	-24.29	-26.57	-28.30	-31.22	-32.27	-32.85	-32.69	-29.00	-16.43	-7.4
0.0	10.90	5.65	1.68	-1.91	-6.10	-9.09	-12.92	-15.92	-18.33	-20.49	-22.95	-23.91	-25.28	-24.47	-22.24	-18.99	-12.43	-2.20	-0.3
0.0	8.55	4.04	0.65	-2.64	-5.65	-8.11	-10.45	-12.65	-14.87	-16.31	-17.92	-17.44	-16.67	-13.74	-7.58	-3.48	1.43	3.72	1.3
0.0	6.83	2.35	0.0	-2.45	-5.15	-7.08	-8.52	-10.26	-11.77	-12.01	-12.35	-11.17	-7.14	0.0	10.90	11.77	7.58	2.01	0.6
0.0	6.02	2.22	-0.57	-2.54	-3.80	-4.99	-6.41	-6.83	-7.97	-8.87	0.0	-4.35	5.65	17.37	20.02	44.12	0.0	0.0	0.0
0.0	5.31	2.11	-0.27	-2.19	-2.51	-3.51	-4.29	-4.59	-5.43	-5.29	-3.70	2.76	19.68	44.60	0.0	0.0	0.0	0.0	0.0
0.0	5.33	2.00	0.0	-1.19	-2.02	-2.16	-2.16	-2.80	-2.47	-2.34	-1.31	10.35	44.73	0.0	0.0	0.0	0.0	0.0	0.0
0.0	5.18	1.95	0.25	-0.24	-0.90	-0.86	-0.43	-0.44	-0.48	-1.40	-0.79	44.68	0.0	0.0	0.0	0.0	0.0	0.0	0.0
0.0	4.61	1.86	0.50	0.0	0.23	0.45	0.45	0.92	0.0	-4.78	-10.90	0.0	0.0	0.0	0.0	0.0	0.0	0.0	0.0
0.0	4.09	1.60	1.00	0.24	0.23	1.17	1.64	2.19	1.46	-5.54	44.26	0.0	0.0	0.0	0.0	0.0	0.0	0.0	0.0
0.0	3.61	1.30	0.50	0.49	0.24	0.49	1.24	1.12	-0.31	-4.27	0.0	0.0	0.0	0.0	0.0	0.0	0.0	0.0	0.0
0.0	2.72	1.30	0.25	0.0	0.24	0.0	-0.25	-1.04	-2.79	-1.57	0.0	0.0	0.0	0.0	0.0	0.0	0.0	0.0	0.0
0.0	1.33	0.52	0.25	0.0	0.0	0.0	-0.24	-0.97	-1.19	-0.46	0.0	0.0	0.0	0.0	0.0	0.0	0.0	0.0	0.0
0.0	0.0	0.0	0.0	0.0	0.0	0.0	0.0	0.0	0.0	0.0	0.0	0.0	0.0	0.0	0.0	0.0	0.0	0.0	0.0

Figure 29. θ - Circular Cutout

APPENDIX C

NOTATION

NOTATION

ϕ = Stress function.

x = Variable distance along the X-axis.

y = Variable distance along the Y-axis.

h = Spacing dimension for a square mesh.

L = Half-width of the plate.

a = Half the major diameter of the ellipse.

b = Half the minor diameter of the ellipse.

σ_x = Stress perpendicular to the X-axis.

σ_y = Stress perpendicular to the Y-axis.

τ_{xy} = Shearing stress in the X-Y plane

σ_n = Uniaxial stress acting on the plate.

σ_{p1} = Major principal stress.

σ_{p2} = Minor principal stress.

θ = Angular orientation of principal stress planes with respect to the X-axis.

C = Constant of integration.